Deuterium Isotope Effects on Permeation and Gating of Proton Channels in Rat Alveolar Epithelium

Thomas E. DeCoursey and Vladimir V. Cherny

From the Department of Molecular Biophysics and Physiology, Rush Presbyterian St. Luke's Medical Center, Chicago, Illinois 60612

ABSTRACT The voltage-activated H^+ selective conductance of rat alveolar epithelial cells was studied using whole-cell and excised-patch voltage-clamp techniques. The effects of substituting deuterium oxide, D_2O, for water, H_2O, on both the conductance and the pH dependence of gating were explored. D^+ was able to permeate proton channels, but with a conductance only about 50% that of H^+. The conductance in D_2O was reduced more than could be accounted for by bulk solvent isotope effects (i.e., the lower mobility of D^+ than H^+), suggesting that D^+ interacts specifically with the channel during permeation. Evidently the H^+ or D^+ current is not diffusion limited, and the H^+ channel does not behave like a water-filled pore. This result indirectly strengthens the hypothesis that H^+ (or D^+) and not OH^- is the ionic species carrying current. The voltage dependence of H^+ channel gating characteristically is sensitive to pH_o and pH_i and was regulated by pD_o and pD_i in an analogous manner, shifting 40 mV/U change in the pD gradient. The time constant of H^+ current activation was about three times slower (τ_{act} was larger) in D_2O than in H_2O. The size of the isotope effect is consistent with deuterium isotope effects for proton abstraction reactions, suggesting that H^+ channel activation requires deprotonation of the channel. In contrast, deactivation (τ_{tail}) was slowed only by a factor $\leq$1.5 in D_2O. The results are interpreted within the context of a model for the regulation of H^+ channel gating by mutually exclusive protonation at internal and external sites (Cherny, V.V., V.S. Markin, and T.E. DeCoursey. 1995. *J. Gen. Physiol.* 105:861–896). Most of the kinetic effects of D_2O can be explained if the pK_a of the external regulatory site is $\sim$0.5 pH U higher in D_2O.

KEY WORDS: ion channels • proton transport • pH • pneumocytes • membrane transport

INTRODUCTION

Voltage-gated H^+ channels conduct H^+ current with extremely high selectivity and exhibit voltage-dependent gating that is strongly modulated by both extracellular and intracellular pH (pH_o and pH_i, respectively).[1] Here we explore the effects of substituting heavy water (deuterium oxide, D_2O), for water (protium oxide, H_2O), on both the conductance and the pH dependence of channel gating. The isotope effect on conductance should provide insight into the mechanism by which permeation occurs. Isotope effects on the regulation by pH (or pD) of the voltage dependence and kinetics of gating provide clues to the possible protonation/deprotonation reactions that have been proposed to play a role in channel gating (Byerly et al., 1984; Cherny et al., 1995).

Several chemical properties of D_2O and H_2O are compared in Table I. From the perspective of this study, the main differences between D_2O and H_2O are: (*a*) the viscosity of D_2O is 25% greater than H_2O, (*b*) the conductivity of H^+ in H_2O is 1.4–1.5 times that of D^+ in D_2O, (*c*) H^+ has a much greater tendency than D^+ to tunnel, (*d*) D^+ weighs twice as much as H^+, and (*e*) D^+ is bound more tightly in D_3O^+ and in many other compounds than is H^+. Three main types of deuterium isotope effects are recognized: general solvent effects and primary and secondary kinetic effects. General solvent isotope effects reflect the different properties of D_2O and H_2O as solvents, such as viscosity or dielectric constant. As seen in Table I, these differences are rather moderate, and their effects are accordingly usually moderate as well. Kinetic isotope effects reflect involvement of protons or deuterons in chemical reactions. Primary kinetic isotope effects occur when H^+ directly participates in a rate-determining step in the re-

Preliminary accounts of this work have been previously reported in abstract form (Cherny, V.V., and T.E. DeCoursey. 1997. *Biophys. J.* 72: A266; DeCoursey, T.E., and V.V. Cherny. 1997. *Biophys. J.* 72:A108).

Address correspondence to Dr. Thomas E. DeCoursey, Department of Molecular Biophysics and Physiology, Rush Presbyterian St. Luke's Medical Center, 1653 West Congress Parkway, Chicago, IL 60612. Fax: 312-942-8711; E-mail: tdecours@rpslmc.edu

[1] *Abbreviations used in this paper:* ΔpD, pD gradient ($pD_o - pD_i$); ΔpH, pH gradient ($pH_o - pH_i$); E_D, Nernst potential for D^+; eff, effective composition of the intracellular solution given the assumptions discussed in *Strategic Considerations*; E_H, Nernst potential for H^+; E_L, either E_H or E_D; g_D, D^+ conductance; g_H, H^+ conductance; GHK, Goldman-Hodgkin-Katz; L^+, either H^+ or D^+; L_3O^+, either H_3O^+ or D_3O^+; pD, the equivalent in D_2O of pH in water; P_d, diffusional water permeability; P_D, permeability to D^+; P_f, osmotic water permeability; P_H, permeability to H^+ calculated with the GHK voltage equation; pH_i, intracellular pH; pH_o, extracellular pH; pL, either pH or pD; P_{osm}, water permeability; P_{TMA}, permeability to TMA^+; OL^-, either OH^- or OD^-; τ_{act}, time constant of activation; τ_{tail}, tail current or deactivation time constant; TMA^+, tetramethylammonium; $TMAMeSO_3$, tetramethylammonium methanesulfonate; V_{hold}, holding potential; V_{rev}, reversal potential; $V_{threshold}$, threshold potential for activating proton currents.

TABLE I

Properties of H_2O and D_2O at 20°C

Property	D_2O/H_2O	Reference
Viscosity (shear)	1.245	Hardy and Cottington, 1949
Viscosity (volume)	1.09	Jarzynski and Davis, 1972
Mobility (conductance)	1.41^{-1}*	Lewis and Doody, 1933
	1.52^{-1}‡	Roberts and Northey, 1974
Dielectric constant	1.005	Schowen, 1977
Dielectric relaxation time	1.28§, 1.29	Collie et al., 1948; Grant and Shack, 1969
Density	1.108	Schowen, 1977
Vapor pressure	1.15^{-1}	Brooks, 1937

We follow Bell's (1973) rationale for expressing isotope effects as a ratio that increases as the magnitude of the isotope effect increases. The ratio of the parameter value in D_2O to that in H_2O is given, but the inverse ratio is given when this results in a ratio >1.0. Note that the mobility values reflect measurements of the mobility of H^+ (or D^+) in the solution, and that the conductivity of a salt solution in H_2O compared with D_2O will differ by a smaller ratio (e.g., 1.17 for KCl, Lewis and Doody, 1933) because the salt will short-circuit the conductivity due to H^+ or D^+ which are present at much lower concentrations. Technical details of the two mobility estimates are discussed on p. 369 of Lengyel and Conway (1983). *Interpolated value. ‡at 25°C. §The ratio given for the dielectric relaxation time, 1.28, is based on the actual measurements of Collie et al. (1948) at 20°C, rather than the "smoothed value" (1.27) given in their Table 6.

action, for example a protonation/deprotonation or H^+ transfer reaction. For example, ionization of a number of bases is typically three to seven times slower in D_2O (Bell, 1973). Secondary isotope effects reflect D^+ for H^+ substitution at some site distinct from the primary reaction center. Secondary kinetic isotope effects tend to be small, 1.02–1.40 (Kirsch, 1977).

The conductivity of H^+ is about five times higher than that of other cations with ionic radii like that of H_3O^+; the limiting equivalent conductivity (λ^0) at 25°C in water is 350 S cm^2/equiv. for H^+ but 73.5 S cm^2/equiv. for NH_4^+ (Robinson and Stokes, 1965). This anomalously high conductivity for H^+ has been ascribed to conduction by a mechanism in which H^+ jumps from H_3O^+ to a neighboring water molecule (Danneel, 1905; Hückel, 1928; Bernal and Fowler, 1933; Conway et al., 1956). H^+ hopping can occur faster than ordinary hydrodynamic diffusion (i.e., bodily movement of an individual H_3O^+ molecule analogous to the diffusion of ordinary ions). After one H^+ conduction event, a structural reorientation of the hydrogen-bonded water lattice is necessary before another proton can be conducted (Danneel, 1905; Bernal and Fowler, 1933; Conway et al., 1956). Proton conduction through channels is believed to occur by an analogous two-step "hop-turn" process through a hydrogen-bonded chain or "proton wire" spanning the membrane (Nagle and Morowitz, 1978; Nagle and Tristram-Nagle, 1983).

The mobility (measured as conductivity) of H^+ in H_2O is 1.41 times that of D^+ in D_2O (Table I); nevertheless, the mobility of D^+ is still 4 times that of K^+ in D_2O (Lewis and Doody, 1933). Thus, D^+ also exhibits abnormally large conductivity, even though tunnel transfer of D^+ is 20 times less likely than for H^+ and one might have expected simple hydrodynamic diffusion of D_3O^+ to play a larger role for D^+, which would accordingly have a conductivity similar to that of other cations (Bernal and Fowler, 1933). Evidently the reorientation of hydrogen-bonded water molecules (the turning step of a hop-turn mechanism) is rate limiting for both H^+ and D^+ conduction. The nature of this rate-determining step has been proposed to be the reorientation of hydrogen-bonded water molecules in the field of the H_3O^+ ion (Conway et al., 1956), "structural diffusion" or formation and decomposition of hydrogen bonds at the edge of the $H_9O_4^+$ complex (i.e., the hydronium ion with its first hydration shell) (Eigen and DeMaeyer, 1958), or more recently, the breaking of an ordinary second-shell hydrogen bond converting $H_9O_4^+$ to $H_5O_2^+$ (Agmon, 1995, 1996). Some such reorganization of hydrogen bonds may also be the rate limiting step in proton translocation across water-filled ion channels such as gramicidin (Pomès and Roux, 1996).

A characteristic feature of voltage-gated H^+ currents is their sensitivity to both pH_o and pH_i. Increasing pH_o and decreasing pH_i shift the voltage-activation curve to more negative potentials in every cell in which these parameters have been studied (reviewed by DeCoursey and Cherny, 1994). This effect of pH is reminiscent of its effects on many other ion channels, which may reflect the neutralization of negative surface charges (see Hille, 1992). However, the magnitude of the pH-induced voltage shifts for H^+ currents has led to the suggestion that protonation of specific sites on or near the channel allosterically modulate gating (Byerly et al., 1984). In alveolar epithelial cells (Cherny et al., 1995), as well as in other cells (DeCoursey and Cherny, 1996*a*; Cherny et al., 1997), the shift produced by internal and external protons (H^+_i and H^+_o) is quite similar, 40 mV/U change in ΔpH, within a large pH range encompassing physiological values. Thus the position of the voltage activation curve can be predicted from the pH gradient, ΔpH, rather than by pH_o and pH_i independently. This behavior was explained by a model (Cherny et al., 1995) in which there exist similar protonation sites accessible from either the internal or external solution, but not both simultaneously. Protonation from the outside stabilizes the closed channel, whereas protonation from the inside stabilizes the open channel. Here we show that H^+ channels are regulated in a similar manner by D^+, but that D^+ binds more tightly to the modulatory sites on the channel molecule.

MATERIALS AND METHODS

Alveolar Epithelial Cells

Type II alveolar epithelial cells were isolated from adult male Sprague-Dawley rats under sodium pentobarbital anesthesia using enzyme digestion, lectin agglutination, and differential adherence, as described in detail elsewhere (DeCoursey et al., 1988; DeCoursey, 1990). Briefly, the lungs were lavaged to remove macrophages, elastase and trypsin were instilled, and then the tissue was minced and forced through fine mesh. Lectin agglutination and differential adherence further removed contaminating cell types. The preparation at first includes mainly type II alveolar epithelial cells, but after several days in culture, the properties of the cells become more like type I cells. No obvious changes in the properties of H^+ currents have been observed. H^+ currents were studied in approximately spherical cells up to several weeks after isolation.

Solutions

Most solutions (both external and internal) contained 1 mM EGTA, 2 mM $MgCl_2$, 100 mM buffer, and $TMAMeSO_3$ added to bring the osmolarity to ~300 mosM, and titrated to the desired pH with tetramethylammonium hydroxide or methanesulfonic acid (solutions using BisTris as a buffer). The pH 8, 9, and 10 solutions contained 3 mM $CaCl_2$ instead of $MgCl_2$. A stock solution of $TMAMeSO_3$ was made by neutralizing tetramethylammonium hydroxide with methanesulfonic acid. Buffers (Sigma Chemical Co., St. Louis, MO), which were used near their pK in the following solutions, were: pH 5.5, pD 6.0 Mes; pH 6.5, pD 7.0 Bis-Tris (bis[2-hydroxyethyl]imino-tris[hydroxymethyl]methane); pH 7.0, pD 7.0 BES (*N,N*-bis[2-hydroxyethyl]-2-aminoethanesulfonic acid); pH 7.5, pD 8.0 HEPES; pH 8.0 Tricine (*N*-tris[hydroxymethyl] methylglycine); pH 9.0, pD 9.0 CHES (2-[N-cyclohexylamino] ethanesulfonic acid); pH 10, pD 10 CAPS (3-[cyclohexylamino]-1-propanesulfonic acid). The pH (or pD) of all solutions was checked frequently.

A series of solutions containing NH_4^+ was made to impose a defined pH gradient across the cell membrane, as described by Grinstein et al. (1994). The principle is that if neutral NH_3 molecules permeate the membrane rapidly enough to approach identical concentrations on both sides of the membrane, then:

$$pH_i = pH_o - \log([NH_4^+]_i/[NH_4^+]_o), \quad (1)$$

because the bath solution is heavily buffered (100 mM buffer) and diffuses freely but the pipette solution (for these measurements) is weakly buffered and diffusion is slowed by the pipette tip. The shift of pH_i occurs because $[H^+]_i = pK_a - \log [NH_4^+]_i/[NH_3]_i$. The extracellular solutions were made with 100 mM HEPES, 2 mM $MgCl_2$, 1 mM EGTA, and various concentrations of $(NH_4)_2SO_4$, at pH 7.5. $TMAMeSO_3$ was added to bring the osmolarity to ~300 mosM. The pipette solution, which was also used externally, included 25 mM $(NH_4)_2SO_4$, 5 mM BES, 2 mM $MgCl_2$, 1 mM EGTA, and $TMAMeSO_3$, brought to pH 7.0 with tetramethylammonium hydroxide.

We assume that when NH_4^+ diffuses from the pipette into the cell, if D_2O is present in the bath (and hence inside the cell) there will be rapid exchange of D^+ for H^+ in NH_4^+, and that therefore efflux of ND_3 will occur, leaving D^+ rather than H^+ behind inside the cell. Deuterons in deutero-ammonia, ND_3, exchange rapidly with protons (Cross and Leighton, 1938).

The osmolarity of solutions was measured with a Wescor 5500 Vapor Pressure Osmometer (Wescor, Logan, UT). Deuterium oxide (99.8% or 99.9%) was purchased from Sigma Chemical Co. A liquid junction potential of ~2 mV was measured between solutions identical except that D_2O replaced H_2O. If water did not permeate the cell membrane, correction for this junction potential would make the transmembrane potential 2 mV more negative. However, as described in Fig. 1, we feel that water permeates the cell membrane, and thus there would be offsetting junction potentials at the pipette tip and bath electrode even in whole cell configuration. Therefore no junction potential correction has been applied.

pD Measurement

The reading taken from a glass pH electrode, pH_{nom}, deviates from the true pD of D_2O solutions by 0.40 U, such that $pD = pH_{nom} + 0.40$ (Glasoe and Long, 1960). Another estimate of this difference is 0.45 ± 0.03 (Dean, 1985), and even more disparate values can be found in early studies. Given the uncertainty about the precise value, we tested our pH meter (Radiometer Ion83 Ion meter; Radiometer, Copenhagen, Denmark) following the approach taken by Glasoe and Long (1960). Our pH meter read 0.402 ± 0.006 (mean ± SD, $n = 3$) higher when 0.01 M HCl was added to H_2O than when added to D_2O. We therefore corrected the pD in D_2O solutions by adding 0.40 to the nominal reading of our pH meter.

Estimation of the pK_a of the Buffers in H_2O and in D_2O

Most simple carboxylic and ammonium acids with pK_a between 4 and 10 have a pK_a 0.5–0.6 U higher in D_2O than in H_2O (Schowen, 1977). We titrated the buffers used in this study at room temperature (20–23°C). 10 mmol of buffer was added to 20 ml of H_2O or D_2O and titrated with 10 N NaOH, or 10 N HCl in the case of Bis-Tris. The resulting contamination of D_2O by the H^+ from the base or acid titrating solutions is <3%. We corrected for this error in two ways. First, we increased the apparent change in pK_a, assuming a linear mole-fraction dependence (cf. Glasoe and Long, 1960), which increased the pK_a in D_2O by ≤0.02 U. We also carried out some titrations using deuterated acids and bases (DCl and NaOD, both from Aldrich Chemical Co, Milwaukee, WI). The results by these two methods were similar. The averages of two to three separate determinations for each buffer are given in Table II.

Electrophysiology

Conventional whole-cell, cell-attached patch, or excised inside-out patch configurations were used. Experiments were done at 20°C, with the bath temperature controlled by Peltier devices and monitored continuously by a thinfilm platinum RTD (resistance temperature detector) element (Omega Engineering, Stamford, CT) immersed in the bath. Micropipettes were pulled in several stages using a Flaming Brown automatic pipette puller (Sutter Instruments, San Rafael, CA) from EG-6 glass (Garner Glass Co., Claremont, CA), coated with Sylgard 184 (Dow Corning Corp., Midland, MI), and heat polished to a tip resistance ranging typically 3–10 MΩ. Electrical contact with the pipette solution was achieved by a thin sintered Ag-AgCl pellet (In Vivo Metric Systems, Healdsburg, CA) attached to a silver wire covered by a Teflon tube. A reference electrode made from a Ag-AgCl pellet was connected to the bath through an agar bridge made with Ringer's solution. The current signal from the patch clamp (List Electronic, Darmstadt, Germany) was recorded and analyzed us-

TABLE II

pK_a of Buffers in H_2O and D_2O

Buffer	pK_a (H_2O)		pK_a (D_2O)		pKa_D-pKa_H
	literature	measured	literature	measured	measured
Mes	6.15*	6.15	—	6.84	0.69
BisTris	6.50‡	6.57	—	7.23	0.66
BES	7.15*	7.10	—	7.79	0.69
HEPES	7.55*	7.57	8.14§	8.22	0.65
Tricine	8.15*	8.15	—	8.81	0.66
CHES	9.30‡	9.34	—	10.03	0.69
CAPS	10.40‡	10.47	—	11.07	0.60

Average pK_a values are for 2–3 paired measurements (H_2O and D_2O done the same day) for each buffer. See MATERIALS AND METHODS for details of titrations and corrections applied (e.g., pK_a values in D_2O were corrected by adding 0.4 to the value read on the pH meter). Literature values and measurements are at room temperature (~20–23°C) except Sigma values are at 25°C. The titration was less accurate at high pH, so the values obtained for CAPS in particular should be considered tentative. The average of all individual pKa_D-pKa_H values in 0.66 ± 0.05 (mean ± SD, n = 17) or excluding the doubtful CAPS data, 0.67 ± 0.04 (n = 14). *Good et al. (1966). ‡Sigma Chemical Company. §Root and MacKinnon (1994).

ing an Indec Laboratory Data Acquisition and Display System (Indec Corporation, Sunnyvale, CA). Data acquisition and analysis programs were written in BASIC-23 or FORTRAN. Seals were formed with Ringer's solution (in mM: 160 NaCl, 4.5 KCl, 2 $CaCl_2$, 1 $MgCl_2$, 5 HEPES, pH 7.4) in the bath, and the zero current potential established after the pipette was in contact with the cell. Inside-out patches were formed by lifting the pipette into the air briefly.

For "typical" families of H^+ currents, pulses were applied in 20-mV increments with an interval of 30–40 s or more, depending on test pulse duration and the behavior of each particular cell. Although 30 s is not long enough for complete recovery from the depletion of intracellular protonated buffer, it represents a compromise aimed at allowing multiple measurements to be made in each cell reasonably close together in time. For some measurements in which only small currents were elicited, such as pulses in 5-mV increments near $V_{threshold}$, a smaller interval between pulses was used, because negligible depletion was expected. We tried to bracket measurements in different solutions whenever possible.

Data Analysis

The time constant of H^+ current activation, τ_{act}, was obtained by fitting the current record by eye with a single exponential after a brief delay (as described in DeCoursey and Cherny, 1995):

$$I(t) = (I_0 - I_\infty) \exp \frac{-(t - t_{delay})}{\tau_{act}}, \quad (2)$$

where I_0 is the initial amplitude of the current after the voltage step, I is the steady-state current amplitude, t is the time after the voltage step, and t_{delay} is the delay. The H^+ current amplitude is ($I_0 - I_\infty$). No other time-dependent conductances were observed consistently under the ionic conditions employed. Tail current time constants, τ_{tail}, were fitted either to a single decaying exponential:

$$I(t) = I_0 \exp \frac{-t}{\tau_{tail}} + I_\infty, \quad (3)$$

where I_0 is the amplitude of the decaying part of the tail current, or to the sum of two exponentials:

$$I(t) = A_1 \exp \frac{-t}{\tau_1} + A_2 \exp \frac{-t}{\tau_2} + A_3, \quad (4)$$

where A_n are amplitudes and τ_n are time constants.

Conventions

We refer to the pL in the format $pL_o//pL_i$. In the inside-out patch configuration the solution in the pipette sets pL_o, which is defined as the pL of the solution bathing the original extracellular surface of the membrane, and the bath solution is considered pL_i. Currents and voltages are presented in the normal sense, that is, upward currents represent current flowing outward through the membrane from the original intracellular surface, and potentials are expressed by defining as 0 mV the original bath solution. Current records are presented without correction for leak current or liquid junction potentials.

As discussed in detail in *Strategic Considerations* and in Fig. 1, when the bath solvent differs from that in the pipette, the effective pH_i (or pD_i) will differ from the nominal value of the pipette solution by ~0.5 U. Therefore, when bath and pipette solvents differ, we provide values for the presumed effective internal H^+ or D^+ concentration, e.g., $pH_{i,eff}$ 6.5 indicates a pD 7.0 pipette solution with any H_2O solution in the bath. The majority of experiments were done with D_2O rather than with H_2O pipette solutions because we wanted the measurements in D_2O to be contaminated as little as possible by H_2O.

RESULTS

Strategic Considerations

The nature of the problem under investigation introduces several complications, which require explanation, as well as a perhaps less-than-obvious approach. Ideally we would like to compare the behavior of the proton conductance in the same cell under identical conditions while varying only the solvent (D_2O or H_2O) on one side of the membrane and keeping pL_o and pL_i constant (pL_x refers to either pH_x or pD_x). However, the high membrane permeability of water means that only symmetrical solvent studies can be contemplated. Less obviously, due to the increased pK_a of buffer in D_2O (Table II), it is impossible to compare directly in the same cell identical pH_o and pD_o by simply changing the external solvent, without at the same time changing pL_i. However, it is desirable to make comparisons in the same cell, because H^+ currents vary substantially from cell to cell. We therefore adopted two strategies. First, we compare currents measured with the same pH or pD gradient (e.g., pH_o 6.5//pH_i 6.5 and pD_o 7.0//pD_i 7.0), because the gradient, ΔpH, appears to be a fundamental determinant of H^+ channel gating (Cherny et al., 1995). This approach has the drawback of comparing the effects of different absolute concentrations of protons and deuterons, and there is some indication that H^+ channel gating kinetics depend on the absolute pH_i, rather than ΔpH alone (DeCoursey and Cherny, 1995). The second approach (see MATERIALS

AND METHODS) overcomes this shortcoming by controlling pH_i by applying a known NH_4^+ gradient (Roos and Boron, 1981), as illustrated by Grinstein et al. (1994). Varying the NH_4^+ gradient allows resetting pH_i (or pD_i) in a cell under whole-cell voltage-clamp, and ideally, comparison of currents at the same pH and pD.

Only symmetrical solvent is possible. In these experiments we varied the solvent in the pipette and bath solutions. Because water has a high membrane permeability, it seemed likely that the solvent in the bath solution would enter the cell much faster than solvent would diffuse from the pipette, and thus the solvent in the bath would also be present in the cell, regardless of the pipette solution. This expectation was tested theoretically and experimentally.

• *How fast does water enter the cell?* A critical question in the interpretation of the data is whether solvent in the bath diffuses across the cell membrane fast enough to dominate the intracellular solution in spite of the presence of the pipette tip which is a continuous source of solvent from the pipette solution. The water permeability, P_{osm}, of planar lipid bilayers or liposomes ranges from 10^{-4} cm/s to 10^{-2} cm/s; P_{osm} in various epithelial cell membranes similarly ranges from 10^{-4} cm/s to $>10^{-2}$ cm/s (Tripathi and Boulpaep, 1989). Because both $HgCl_2$-sensitive and $HgCl_2$-insensitive water channels occur in lung tissue (Folkesson et al., 1994; Hasegawa et al., 1994), it is likely that P_{osm} is relatively high in alveolar epithelial cells, at least in situ. Osmotic water permeability (P_f) is 1.7 ± 10^{-2} cm/s and diffusional water permeability, P_d, is 1.3 ± 10^{-5} cm/s across the alveoli of intact mouse lung (Carter et al., 1996). However, P_d was probably grossly underestimated because of unstirred layer effects (Finkelstein, 1984; Carter et al., 1996). We calculated the steady-state distribution of normal or heavy water when one species was in the pipette solution and the other in the bath solution. The compartmental diffusion model used has been described in detail previously (DeCoursey, 1995), and simplifies the calculation by placing the pipette tip at the center of a spherical cell. The diffusion coefficient of H_2O was taken as 2.1×10^{-5} cm^2/s (Robinson and Stokes, 1965), the pipette tip was assumed to have a diameter of 1.0 μm, the cell diameter was 20 μm, and we assume that D_2O and H_2O have similar membrane permeabilities (Perkins and Cafiso, 1986; Deamer, 1987; Gutknecht, 1987). A range of P_{osm} was assumed. For $P_{osm} > 10^{-3}$ cm/s the membrane presented essentially no barrier to diffusion, and the solvent in the bath was the main solvent inside the cell. Nevertheless, because the pipette is a constant source, there is always a finite concentration of the pipette solvent. For the pipette tip at the center of a 20 μm diameter cell, the limiting submembrane concentration at infinite P_{osm} is ~2% due to that in the pipette. Lowering P_{osm} to 10^{-4} cm/s caused the membrane to become a significant diffusion barrier, with the steady-state concentration of solvent near the inside of the membrane 24% due to the pipette and 76% due to the bath. The fraction of solvent near the membrane originating in the pipette would be larger in a smaller cell but would be smaller if the pipette tip diameter were smaller. In conclusion, the pipette solvent is present in the cell at significant levels only for a quite conservative estimate of P_{osm}, and in all likelihood the solvent in the bath permeates the membrane rapidly enough that most of the solvent near the membrane originated in the bath. We therefore assume that the membrane is exposed to nearly symmetrical solvent, with a finite but small contribution from the pipette.

• *What is the pL (pH or pD) inside the cell?* The actual pL_i can be deduced from knowledge of pL_o and the reversal potential, V_{rev}. In the experiment illustrated in Fig. 1, the pipette contained pD 7.0 solution, and the tail current reversal potential, V_{rev}, was measured in several different bath solutions. V_{rev} was near 0 mV when the bath contained pD 7.0 (Fig. 1 *A*) or pH 6.5 (Fig. 1 *C*), and was −27 mV at pH_o 7.0 (Fig. 1 *B*). In eight cells, V_{rev} was 29.9 ± 4.5 mV (mean ± SD) more negative at pH_o 7.0 than at pD_o 7.0, both with pD_i 7.0. Reversal near 0 mV is expected for symmetrical pD 7.0//7.0. Why was V_{rev} near 0 mV at pH_o 6.5 but not at pH_o 7.0, under nominally symmetrical bi-ionic conditions? The explanation arises from the fact that many molecules bind D^+ more tightly than H^+. Most simple carboxylic and ammonium acids with pK_a between 4 and 10, including buffers, have a pK_a 0.5–0.6 U higher in D_2O than in H_2O (Schowen, 1977). We confirmed this generalization by titrating the buffers used in this study in both H_2O and D_2O and found pK_a shifts ranging 0.60–0.69 U (Table II). Fig. 1 *D* illustrates diagrammatically the effect of this pK_a difference on a cell studied in the whole-cell configuration. The cell nominally contains the pipette solution with its buffer titrated to some pH or pD, in this example pD 7.0. If the solvent in the bath differs from that in the pipette, the bath solvent will replace the pipette solvent inside the cell, as discussed above. Because H^+ has a lower affinity for buffer than does D^+, fewer H^+ will be bound to buffer than were D^+, and hence the actual pH_i will be lower by ~0.5 U than was the pD of the pipette solution. This is true regardless of the actual value of pH_o, because it results from the solvent dependence of the pK_a of the buffer. The chart in Fig. 1 summarizes the experiment illustrated. Given the bath and pipette solutions, the observed V_{rev} agrees well with E_H calculated with the assumptions that (*a*) the solvent in the bath completely replaces that in the cell, and (*b*) the effective pH_i will be ~0.5 U lower than pD in the pipette when H_2O replaces D_2O in the bath. By similar logic, when H_2O is in

the pipette solution and D_2O is in the bath, the actual pD_i will be ~0.5 U higher than pH_i with H_2O in the bath.

• *V_{rev} measurements are consistent with high water permeability and the 0.5 U pK_a correction for intracellular buffer in D_2O.* We proposed above that the bath solvent will "fill" the cell regardless of the pipette solvent and that when the bath solvent differs from that in the pipette, pL_i will change by ~0.5 U from its nominal value. To a first approximation these assumptions seem reasonable, but two possible sources of error should be considered. First, some finite fraction of solvent in the cell is derived from the pipette. We could not determine from

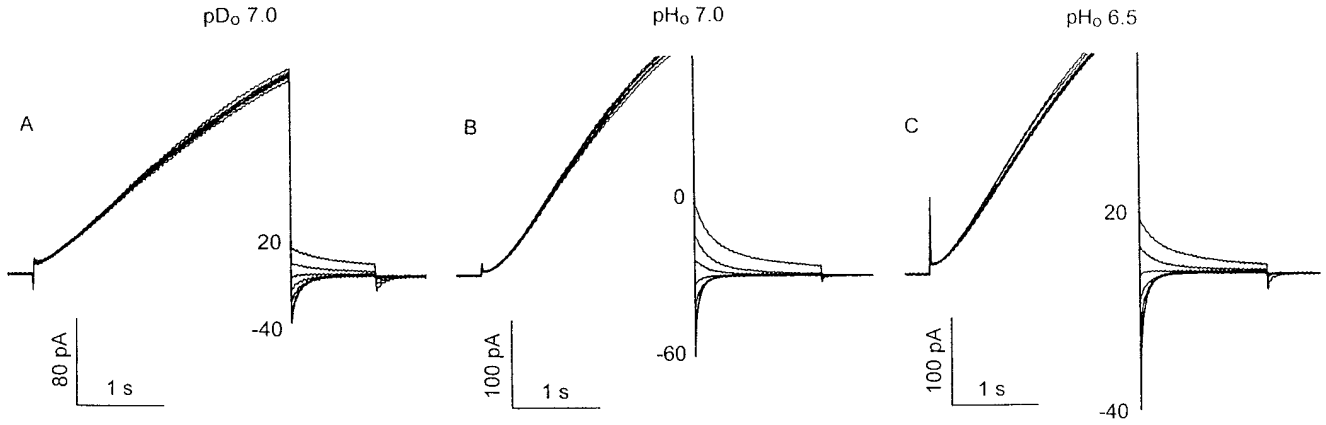

	BATH		CELL		PIPETTE		(mV)	
	solvent	pL	solvent	pL	solvent	pL	E_L	V_{rev}
A	D_20	pD 7.0	D_20	pD 7.0	D_20	pD 7.0	0	+3
B	H_20	pH 7.0	H_20	pH 6.5	D_20	pD 7.0	-29	-27
C	H_20	pH 6.5	H_20	pH 6.5	D_20	pD 7.0	0	+1

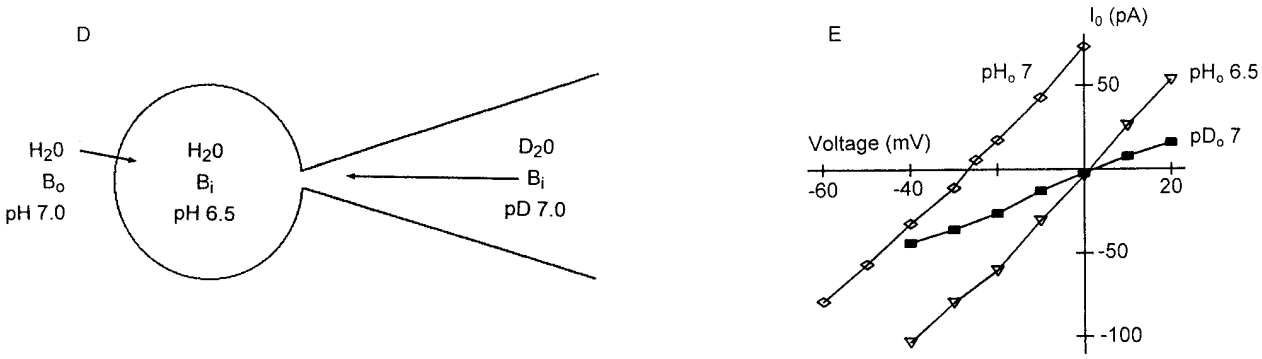

FIGURE 1. The solvent in the bath replaces the solvent in the cell. Measurement of the tail current reversal potential, V_{rev}, is illustrated in a cell studied with a pipette solution containing D_2O at pD 7.0. The bath solution was D_2O at pD 7.0 (*A*), or H_2O at pH 7.0 (*B*) or pH 6.5 (*C*). (*D*) Schematic diagram of a didactic experiment in which the pipette solution is D_2O at pD 7.0 and the bath contains H_2O at pH 7.0 (or pH 6.5). The solvent in the bath permeates the membrane and fills the cell faster than the pipette solvent diffuses into the cell. Buffered pipette solution enters the cell, but H_2O replaces D_2O, and the effective pH_i is 0.5 U lower than was the original pD of the pipette solution. In the table the composition of the bath and pipette solutions, and the presumed effective composition of the solution in the cell is given, and a comparison of observed V_{rev} values with the Nernst potential, E_L. E_L was calculated assuming that the bath solvent fills the cell and that the pK_a of all buffers is 0.5 U higher in D_2O than in H_2O (see text for details). (*E*) Instantaneous current-voltage relationships for the measurements in parts *A* (■), *B* (◇), and *C* (▽). The amplitude of a single exponential fitted by eye to the tail current at each voltage is plotted. V_{rev} was determined by interpolation.

our data the extent of this "contamination." Second, we assume that the buffer pK_a increases exactly 0.5 U when D_2O replaces H_2O, although the true change may be slightly higher and may differ for different buffers. Our titration of several buffers used (Table II) revealed an average pK_a shift of 0.67 U in D_2O. To test the adequacy of our approximation of a 0.5 U shift, we compared the value for V_{rev} measured in the same cell in D_2O and in H_2O at 0.5 U lower pL_o. The difference in V_{rev} averaged 2.9 ± 0.7 mV (mean ± SEM, n = 21) for pD_o 6.0–pH_o 5.5, pD_o 7.0–pH_o 6.5, and pD_o 8.0–pH_o 7.5. We could not detect any significant difference between buffers in this respect. By this measure the actual pH_i may be ~0.05 U more acidic than our assumed value, i.e., pH_i may be 0.55 U lower than pD_i. However, considering that the slope of the V_{rev} vs. ΔpH relationship in water was 52.4 mV (Cherny et al., 1995) compared with 58.2 mV for E_H, possibly indicating a ~10% attenuation of the ΔpH applied across the membrane, one might suggest that the change in buffer pK_a should also be attenuated by 10% for internal consistency.

A complementary comparison can be made between V_{rev} measured in the same bath solution, but with H_2O or D_2O in the pipette solution. At pD_o 7, V_{rev} averaged +4.5 ± 1.2 mV (mean ± SEM, n = 4) with pH_i 6.5 and +4.3 ± 0.8 mV (n = 12) with pD_i 7. At pH_o 6.5, V_{rev} averaged +2.0 ± 1.6 mV (n = 4) with pH_i 6.5, and +0.5 ± 1.1 mV (n = 10) with pD_i 7. Thus, no systematic difference was observed in V_{rev} with D_2O or H_2O in the pipette. Together these data support the validity of the assumptions used to interpret these experiments.

Reversal Potential of D^+ Currents

Values of V_{rev} obtained from tail current measurements, such as those illustrated in Fig. 1, *A–C*, in bilateral D_2O are plotted as a function of the pD gradient in Fig. 2. In most experiments, V_{rev} was slightly positive to the calculated Nernst potential for D^+, E_D (*dark line*), reminiscent of the small positive deviations of V_{rev} from E_H reported in most studies of H^+ currents. Most of the data points for each pD_i parallel E_D, clearly establishing the selectivity of this conductance for D^+. The largest deviation occurred at pD_o 10//pD_i 8. Parallel experiments in H_2O solutions (not shown) produced a similar but more exaggerated result—V_{rev} followed E_H closely up to pH_o 8, with a smaller shift at pH_o 9, and no further shift at pH_o 10. The simplest interpretation of this result is that at high pH_o there is a loss of control over pH_i.

A more traditional but less attractive interpretation of the deviations of V_{rev} from E_D is that the selectivity of the conductance for D^+ is not absolute, and that at high pL the permeability to some other ion (e.g., TMA^+) is increased. However, the observed deviations are not consistent with a constant permeability of

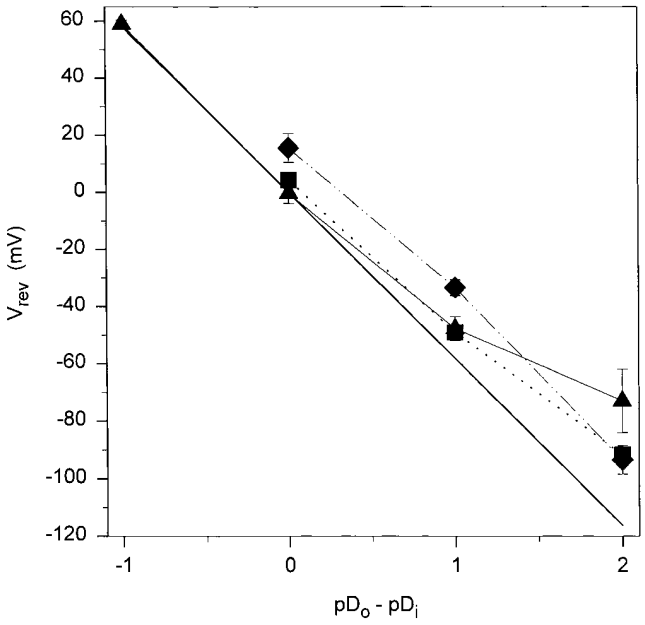

FIGURE 2. Reversal potentials, V_{rev}, measured in bilateral D_2O. V_{rev} was estimated from tail currents as illustrated in Fig. 1 *A–C*, and *E*. Symbols indicate mean ± SD of 2–12 measurements (48 in all) with pD_i 6.0 (◆), pD_i 7.0 (■), or pD_i 8.0 (▲), and pD_o 6–10. The dark line shows the Nernst potential.

TMA^+ relative to D^+, because they were roughly the same at a given pD gradient, ΔpD, at various absolute pD. Thus, the ratio P_{TMA}/P_D calculated using the GHK voltage equation was 2×10^{-7}, 2×10^{-8}, and 5×10^{-9} at pD · 6, pD · 7, or pD · 8, respectively, all at ΔpD = 2.0. Barring a bizarrely concentration-dependent permeability ratio, it appears that the conductance is extremely selective for D^+ (or H^+), with a relative permeability $>10^8$ greater for D^+ than for TMA^+.

Behavior of the Proton Conductance in D_2O

Effects of changes in pD_o. After complete replacement of water with heavy water, D^+ currents behaved qualitatively like H^+ currents in normal water. Typical families of currents are illustrated in Fig. 3, with pD_i 6 and pD_o 8, 7, or 6. At relatively negative potentials only a small time-independent leak current was observed. During depolarizing pulses a slowly activating outward current appeared. The current has a sigmoid time course, and activation was faster at more positive potentials. Decreasing pD_o produced two distinct effects on the currents. The voltage at which the conductance was first activated, $V_{threshold}$, became more positive by about 40 mV/U decrease in pD_o, and the rate of current activation became slower. This shift in the position of the voltage-activation curve is more apparent in Fig. 4. The currents measured at the end of 8-s pulses are plotted (*solid symbols*), as well as the amplitude extrapolated

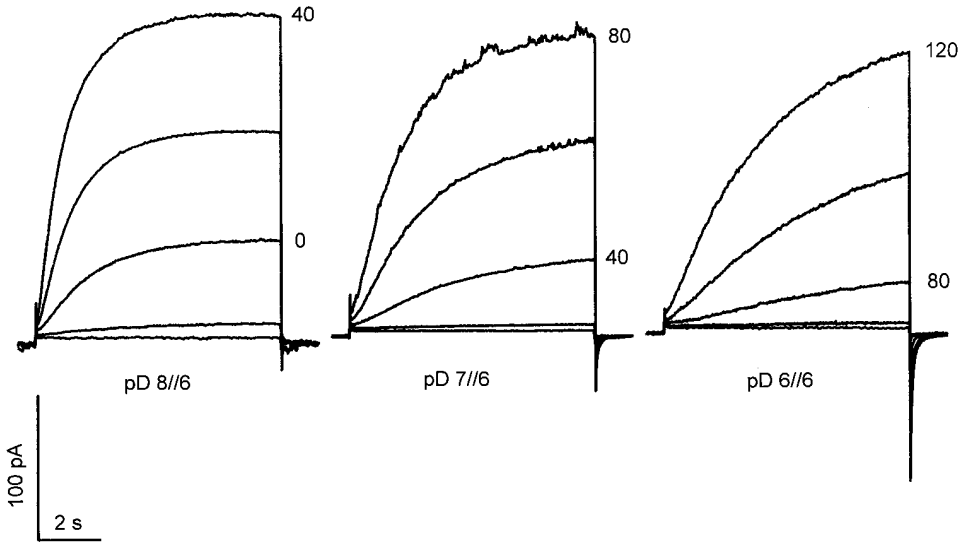

FIGURE 3. The effect of pD_o on D^+ currents is similar to the effect of pH_o on H^+ currents. Families of currents are shown for a cell studied with pD_i 6.0, and pD_o 8.0 (*A*), pD_o 7.0 (*B*), and pD_o 6.0 (*C*). Calibration bars apply to all three families. The holding potential, V_{hold}, was −60 mV (*A*) or −40 mV (*B* and *C*). Illustrated currents are for pulses applied in 20-mV increments to −40 through +40 mV (*A*), 0 to +80 mV (*B*), and +40 to +120 mV (*C*). Filter, 100 Hz.

from a single-exponential fit to the rising phase (*open symbols*). This latter value corrects for the fact that the currents did not always reach steady state by the end of the pulses, as well as correcting for any time-independent leak current. In this example, and in other experiments, the shift in the current-voltage relationship was very nearly 40 mV/U decrease in pD_o. These effects are quite similar to those of changes in pH_o in water (Cherny et al., 1995).

Another effect of changes in pD_o evident in Fig. 3 is that the conductance was activated more slowly at lower pD_o. The time course of activation of H^+ or D^+ currents was fitted by a single exponential after a delay (Eq. 2). In some cases the fit was good, as in the example shown in the inset to Fig. 5, but sometimes the time course was more complex, with fast and slow components. Deviations from an exponential time course seemed most pronounced at large positive voltages and when there was a large pD gradient. Activation time constants, τ_{act}, in the same cell at pD_o 8, 7, and 6 are plotted in Fig. 5. At each pD_o τ_{act} is clearly voltage dependent, decreasing with depolarization. Lowering pD_o appears to shift the τ_{act}-*V* relationship to more positive potentials and upwards, slowing activation in addition to shifting the voltage dependence. Similar results were obtained in other cells. Although the magnitude of τ_{act} varied from cell to cell, the effects of changes in pD_o in each cell were quite similar to those illustrated.

Effects of changes in pD_i. The effects of pD_i on D^+ currents were studied both in whole-cell experiments and in excised patches. Studying patches allows a direct comparison in the same membrane. Fig. 6 illustrates D^+ currents in an inside-out patch at pD_o 8.0 and pD_i 6.0 (*A*) or pD_i 7.0 (*B*). In this and in several other patches $V_{threshold}$ was shifted by about −40 mV/U decrease in pD_i. Time-dependent outward current first appeared at −40 mV at pD_i 6.0 and at 0 mV at pD_i 7.0. The small amplitude of most patch currents in D_2O limits the quantitative accuracy of any conclusions. However, the conductance approximately doubled when pH_i was reduced 1 U, comparable with the 1.7-fold increase/U decrease in pH_i reported previously in inside-out patches (DeCoursey and Cherny, 1995). It is also obvious that activation was much faster at lower pD_i.

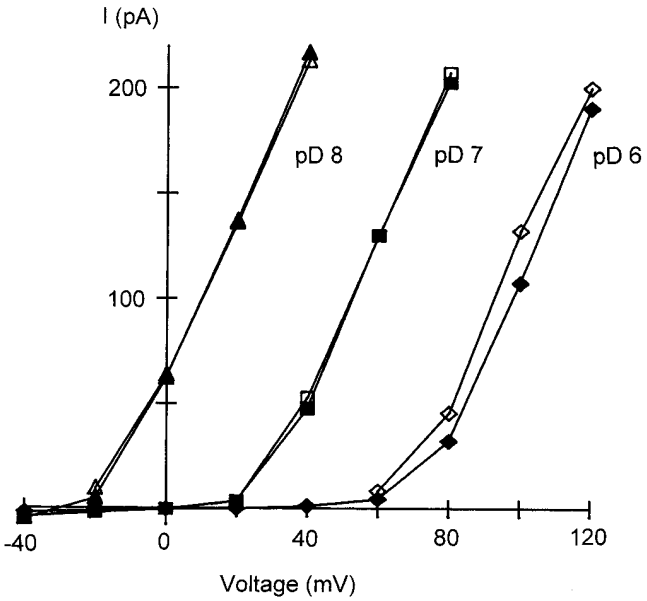

FIGURE 4. Dependence of the current-voltage relationship on pD_o. The current amplitude measured at the end of the 8-s pulses illustrated in Fig. 3 *A–C* is plotted, without leak correction (*solid symbols*). Also plotted is the amplitude of a single exponential (Eq. 2, Fig. 5) fitted to the same currents (*open symbols*). This idealized amplitude is increased over the raw value when the currents did not reach steady-state during the pulses but reduced by the leak correction inherent in this procedure.

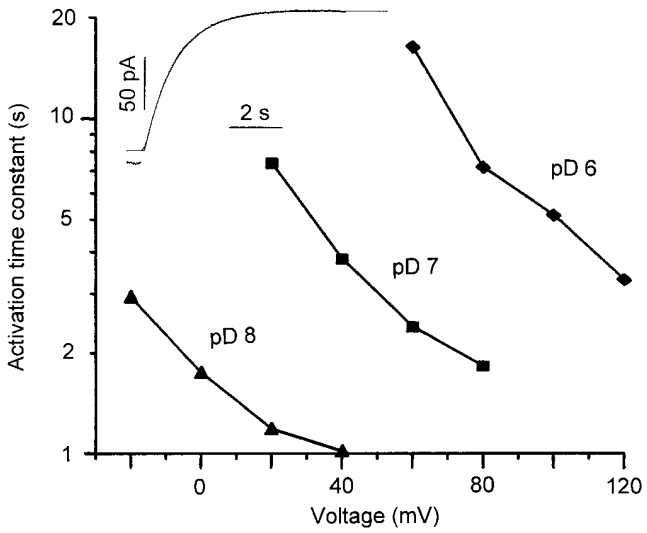

FIGURE 5. Time constant of activation, τ_{act}, measured in the same cell as in Figs. 3 and 4, at pD_o 8, 7, and 6, with pD_i 6.0. Inset shows the fit of a single exponential after a delay to the D^+ current (shown as points) at +20 mV at pD_o 8//pD_i 6 in this cell. The amplitude was 135 pA, τ_{act} was 1.17 s, and the delay was 116 ms.

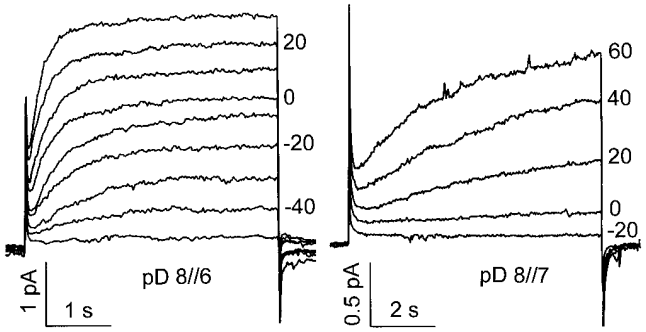

FIGURE 6. D^+ currents in an inside-out patch, illustrating the effects of changes in pD_i. The pipette contained pD 8.0 solution, and the bath either pD 6.0 (*A*) or pD 7.0 (*B*). Superimposed in *A* are currents during two runs: from V_{hold} = −60 to −40 mV through +20 mV in 20-mV increments, and from V_{hold} = −70 to −50 mV through +30 mV in 20-mV increments, as indicated. (*B*) Currents in the same patch at pD_o 8//pD_i 7. V_{hold} was −40 mV, and pulses were to −20 mV through +60 mV in 20-mV increments, as indicated. Filter, 20 Hz.

The effects of changes in pD_i in whole-cell experiments were explored in individual cells by varying the NH_4^+ gradient across the cell membrane (MATERIALS AND METHODS). Fig. 7 illustrates families of D^+ currents in a cell at two NH_4^+ gradients. In each case pD_o was 7.5, but pD_i decreased as the NH_4^+ in the bath was lowered. With a 1//50 NH_4^+ gradient (*A*) V_{rev} was −66 mV, and with a 15//50 NH_4^+ gradient (*B*) V_{rev} was −27 mV. On the basis of this change in V_{rev}, pD_i was ~0.7 U lower in *A* than in *B*. At lower pD_i the currents activated more rapidly and the conductance appeared to be increased. Qualitatively similar effects of changes in pH_i were seen in H_2O solutions at various NH_4^+ gradients in alveolar epithelium (not shown) and in macrophages (Grinstein et al., 1994).

Deuterium Isotope Effects on H^+ (D^+) Currents

Families of currents in the same cell in H_2O and D_2O are illustrated in Fig. 8. To keep ΔpL approximately constant, we compared pH_o 6.5//$pH_{i,eff}$ 6.5 and pD_o 7// pD_i 7 (Fig. 8, *A* and *B*, respectively). In D_2O the currents are smaller and activate more slowly.

Voltage-gated current amplitude. The average ratios of the current measured in individual cells both in effectively symmetrical H_2O and symmetrical D_2O are plotted in Fig. 9. The "steady-state" current amplitudes were obtained by extrapolation of single exponential fits (Eq. 2). At all potentials the currents were substantially larger in H_2O. The ratio decreased at more positive potentials, but two sources of error would tend to cause a voltage-independent effect to deviate in this direction. First, during large depolarizations there is depletion of protonated (or deuterated) buffer from the cell, which tends to reduce the currents in a current-dependent manner. Because the currents were larger in H_2O, there would be more attenuation than in D_2O. Second, to the extent that the position of the voltage-activation curve may be shifted slightly positive in D_2O relative to H_2O (e.g., see Figs. 10 and 11), a smaller fraction of the total conductance would be activated in D_2O, and this would mainly affect smaller depolarizations to the steep part of the g_H-V relationship. Thus, it is not clear whether this effect was voltage dependent. The average ratio at +80 and +100 mV was 1.92 at pD 8 compared with pH 7.5, 1.91 at pD 7 compared with pH 6.5, and 1.65 at pD 6 compared with pH 5.5. In summary, the current carried by H^+ through proton channels is about twice as large as that carried by D^+.

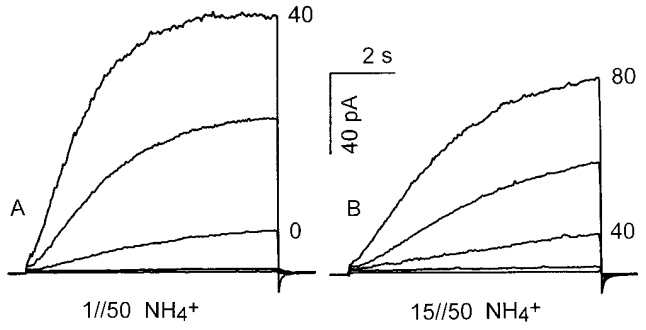

FIGURE 7. Appearance of whole-cell D^+ currents at different pD_i with constant pD_o 7.5. (*A*) The NH_4^+ gradient was 1//50 and V_{rev} was −66 mV. From V_{hold} = −60 mV pulses were applied in 20-mV increments at 30-s intervals to −40 through +40 mV. (*B*) In the same cell at a 15//50 NH_4^+ gradient, V_{rev} was −27 mV. From V_{hold} = −40 mV, pulses were applied to 0 through +80 mV. Calibration bars apply to both families.

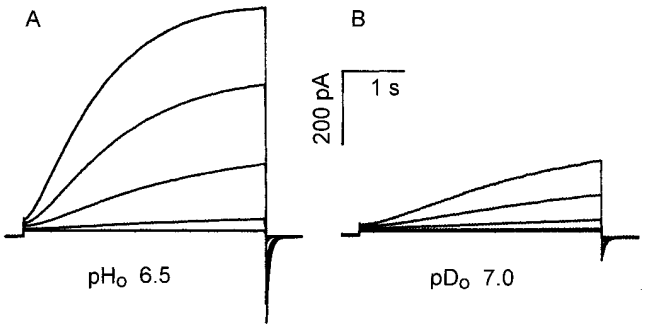

FIGURE 8. Families of currents in the same cell at pH_o 6.5 (*A*) and pD_o 7.0 (*B*). The pipette contained pD 7.0 solution, and we assume that with H_2O in the bath the membrane in *A* effectively "sees" pH_o 6.5//$pH_{i,eff}$ 6.5. In both parts, pulses were applied from V_{hold} = −40 mV in 20-mV increments up to +100 mV. The observed V_{rev} in this cell was −1 mV (*A*) and +3 mV (*B*). Filter, 100 Hz; families recorded 66 and 80 min after achieving whole-cell configuration.

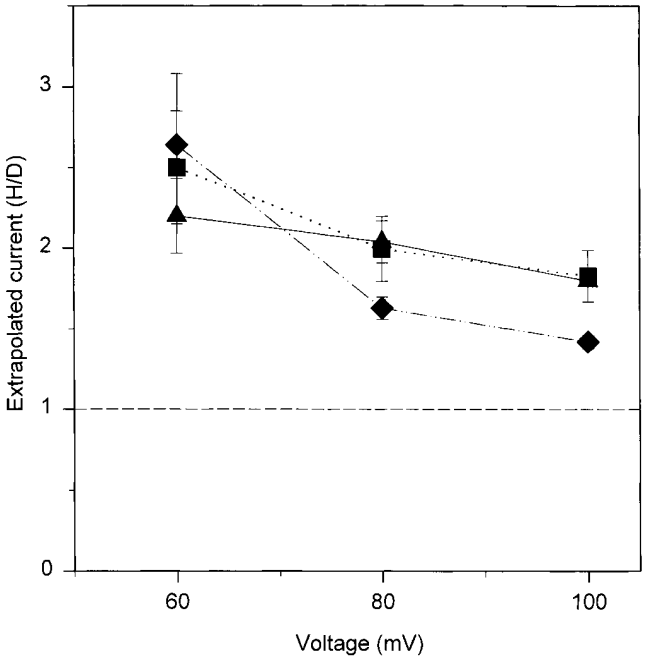

FIGURE 9. Ratio of the extrapolated or "steady-state" current amplitude in H_2O to that in D_2O in the same cell at the corresponding pL. Symbols show the mean ± SEM of the ratio of pD_o 8 to pH_o 7.5 in 3–5 cells (▲), pD_o 7 to pH_o 6.5 in 8–10 cells (■), and pD_o 6 to pH_o 5.5 in 4 cells (◆). Corresponding τ_{act} ratios from the same data set are plotted in Fig. 13. The steady-state current amplitude was obtained by extrapolation of a single exponential (after a delay) fitted to the outward currents (Eq. 2). The effective pL_i in each case is 0.5 U higher in D_2O than in H_2O (see *Practical Considerations*). The only significant differences between mean values were at +80 mV and +100 mV at pD_o 6 vs. pD_o 8 ($P < 0.05$).

Comparison of the g_H-voltage and g_D-voltage relationships. In symmetrical D_2O the conductance-voltage relationship shifted about 40 mV/U change in ΔpD just as in H_2O. However, the absolute voltage dependence might be different in the two solvents. To address this possibility we compared similar ΔpH and ΔpD in the same cell, varying the NH_4^+ gradient to regulate pL_i. Fig. 10 illustrates a typical experiment. Measurements were made in D_2O (*filled symbols*) and in water (*open symbols*) at 1//50 NH_4^+ (▲), 3//50 mM NH_4^+ (◆), and 15//50 mM NH_4^+ (■). At each NH_4^+ gradient, the g_D-V relation was shifted 10–15 mV positive to the corresponding g_H-V relation. Moreover, V_{rev} was consistently more positive in D_2O at any given NH_4^+ gradient. Apparently NH_4^+ gradients were less effective at clamping pL_i in D_2O, perhaps reflecting the higher viscosity of D_2O (Table I), or the higher pK_a of NH_4^+ in D_2O (Lewis and Schutz, 1934)—at any given pL there would be a smaller concentration of neutral ND_3 than NH_3 available to permeate the membrane. The cytoplasmic acidifying power of 3 mM NH_4^+ in D_2O might be roughly equivalent to that of 1 mM NH_4^+ in H_2O, as was observed in the experiment illustrated in Fig. 10, if the neutral form were present at equal concentration, because the NH_4^+ gradient changes pL_i in a dynamic manner through a sustained flux of neutral NH_3. Indeed, Grinstein et al. (1994) found that methylamine$^+$, with a pK_a 10.19 compared with 9.24 for NH_4^+ (Dean, 1985), acidified the cytoplasm more slowly given the same gradient than did NH_4^+. If one assumes that V_{rev} accurately reflects pL_i then correcting for the difference in V_{rev} reduces the average shift in D_2O (compared with H_2O) to only ~5 mV. Scaling the D_2O data up to correct for the smaller limiting conductance further reduces the size of the shift. A residual shift of a few mV cannot be ruled out, but any such shift is not large, and it is possible that there is no shift.

Fig. 10 also shows that the conductance near threshold potentials changed *e*-fold in 4–5 mV at each NH_4^+ gradient. We could not detect any difference in this limiting slope in D_2O and H_2O. Measured at 10^{-2} to 10^{-3} of its maximal value, the conductance changed *e*-fold in 4.65 ± 0.16 mV (mean ± SEM, n = 22) in D_2O and H_2O combined; the lines drawn through the data in Fig. 10 illustrate this average slope. This slope corresponds with the translocation of 5.4 charges across the membrane during gating, which should be considered a lower bound for the actual gating charge movement.

Finally, examination of the limiting maximum conductance at large depolarizations (Fig. 10) reveals that over the range of pL_i studied, the conductance was about twice as large in H_2O as in D_2O. This result is an important corroboration of the conclusion drawn from Figs. 8 and 9, because those comparisons were at ~0.5 U different absolute pL_i. The higher conductance in H_2O than in D_2O in Fig. 10 cannot be ascribed to different pL_i and must reflect a fundamental difference in the rate at which D^+ and H^+ permeate the channel.

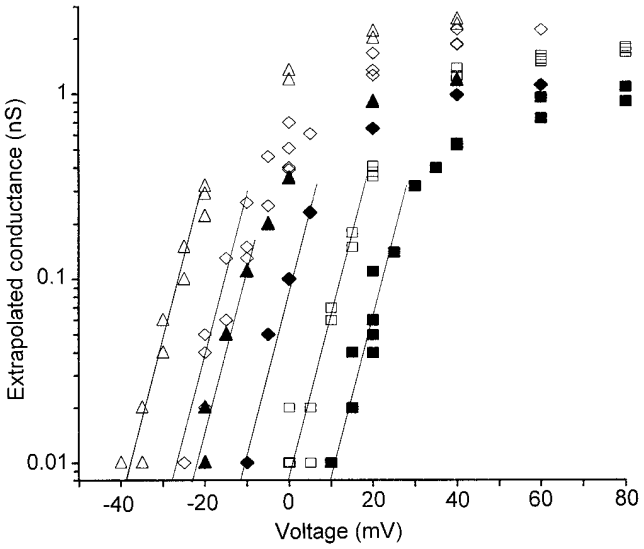

FIGURE 10. Steady-state voltage-gated conductance in D_2O (*filled symbols*) or H_2O (*open symbols*) in various NH_4^+ gradients in the same cell at pL_o 7.5. The NH_4^+ gradient was 15//50 mM (*squares*), 3//50 mM (*diamonds*), and 1//50 mM (*triangles*). The lines show the average limiting slope of 4.65 mV/*e*-fold change in conductance (see text). The chord conductance was calculated using V_{rev} measured in each solution. Currents recorded during voltage pulses 4–16 s long were fitted with a single rising exponential after a delay (Eq. 2). The amplitude of the exponential component is plotted. Longer pulses were used in D_2O and for small depolarizations above threshold, where τ_{act} was larger. Measurements were made in some solutions two or three different times during the experiment. The average V_{rev} (of 1–3 determinations) in H_2O and D_2O, respectively, at each NH_4^+ gradient were: 15//50 (−32 mV, −27 mV), 3//50 (−65 mV, −58 mV), and 1//50 (−78 mV, −67 mV). The protons in 50 mM NH_4^+ contaminate the D_2O by only ~0.2%.

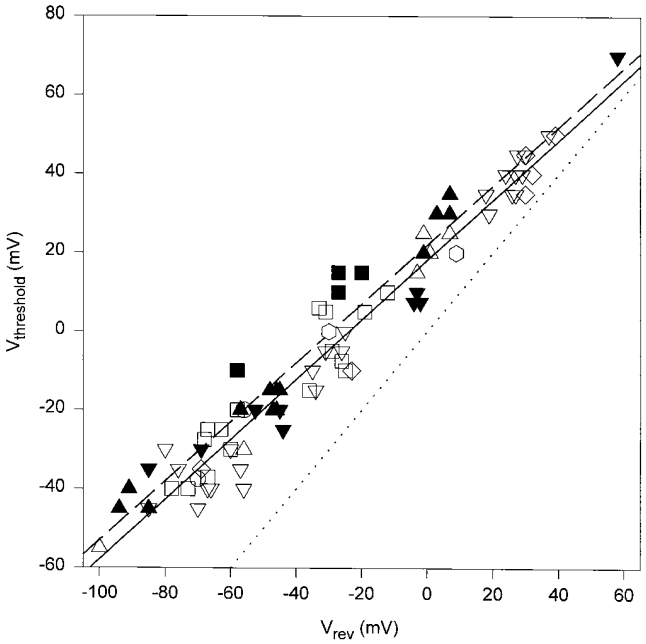

FIGURE 11. The potential at which clearly time-dependent outward current was detected, $V_{threshold}$, is plotted as a function of V_{rev} measured in the same cell and the same solution. Only data in which $V_{threshold}$ was examined using voltage increments of 5 mV or less are included. Open symbols indicate measurements with H_2O in the bath; filled symbols indicate measurements with D_2O. Pipette solutions are indicated by the shape of the symbol: pD 7.0 (△), pD 8.0 (▽), pD 9.0 (*open hexagons*), pH 7.5 (◇), pH 5.5 (○), 50 mM NH_4^+ (□). The data with H_2O in the bath are considered to be essentially symmetrical H_2O (see *Strategic Considerations*), and those with D_2O in the bath symmetrical D_2O. The lines show the results of linear regression of the H_2O data (*solid line*), $r = 0.963$, slope = 0.760, y-intercept = 18.1 mV. The D_2O data (*dashed line*) were described by $r = 0.926$, slope = 0.750, y-intercept = 22.0 mV. Dotted line shows $V_{threshold} = V_{rev}$ illustrating that $V_{threshold}$ is positive to V_{rev} over the entire physiological range.

Relationship between $V_{threshold}$ and V_{rev}. The potential at which the H^+ conductance is first activated by depolarization, $V_{threshold}$, is plotted in Fig. 11 as a function of V_{rev} in H_2O (*open symbols*) and in D_2O (*filled symbols*). Data obtained at pH_o 6.5–10.0 and pD_o 7–10 are included, as well as from experiments in which pL_i was changed by varying the NH_4^+ gradient across the membrane. The data describe a remarkably linear relationship, with no suggestion of saturation at either extreme. The data for effectively symmetrical H_2O and D_2O fitted independently by linear regression yielded identical slopes (0.76 for H_2O and 0.75 for D_2O). Thomas (1988) observed a similarly linear relationship between E_H and V_{rev} in snail neurons, over a range of pH_i ~7–8. This result shows clearly that the fundamental determinant of the position of the voltage-activation curve of the g_H is the pH gradient across the membrane, as was concluded previously (Cherny et al., 1995).

The regression line in Fig. 11 for D_2O is shifted 3.9 mV from that for H_2O, indicating a more positive $V_{threshold}$ for a given V_{rev}. This small shift may be an artifact resulting from the greater difficulty in detecting small currents in D_2O because the conductance is smaller and activation is slower. In any case, there was little or no solvent dependence of the relationship between V_{rev} and $V_{threshold}$, suggesting the position of the voltage-activation curve of the proton conductance is fixed in a very similar manner by ΔpD as by ΔpH.

Deuterium slows channel opening. The time-course of H^+ or D^+ current activation during depolarizing pulses was fitted by a single exponential after a delay to obtain τ_{act}, as was shown in the inset in Fig. 5. Mean values for τ_{act} at various pD (*solid symbols*) and pH (*open symbols*) are plotted in Fig. 12, all for ΔpL = 0. It is unclear from these data whether there might be some effect of the absolute value of pL on τ_{act}. However, all the mean τ_{act} values in D_2O are slower at each potential than any of the values in H_2O. The average of the ratios at all potentials ≥60 mV of the mean τ_{act} values in D_2O to H_2O at 0.5 U lower pL_i was 3.21 at pD 8, 3.19 at pD 7, and 2.96 at pD 6. In summary, D_2O slows τ_{act} by about threefold.

Because there was substantial variability of τ_{act} from one cell to another, comparisons were also made in individual cells at effectively symmetrical pH or pD. The average ratio of τ_{act} in D_2O to that in H_2O plotted in Fig. 13 reveals that τ_{act} was 2.0–3.6 times slower in D_2O. The slowing was not noticeably voltage dependent. There is a suggestion that the slowing effect was greater at higher pD (or pH). If the ratios at all voltages in each solution are averaged, the slowing effect was 2.17 at pD 6 compared with pH 5.5, 3.06 at pD 7 compared with pH 6.5, and 3.21 at pD 8 compared with pH 7.5. The solid symbols include only cells studied with D_2O pipette solutions, the open squares show data from cells with H_2O in the pipette. The slowing of τ_{act} by D_2O appears to be attenuated in these cells, possibly reflecting the small amount of H_2O inside the cell, although the difference is not significant. In summary, D_2O slows τ_{act} about threefold, and this effect appears to be voltage independent.

Deuterium does not strongly affect deactivation kinetics. The channel closing rate was examined by fitting the time course of the decay of tail currents (MATERIALS AND METHODS), such as those illustrated in Fig. 1, *A–C*. The average values of τ_{tail} obtained in effectively symmetrical solutions are plotted in Fig. 14. There is a suggestion in the data that τ_{tail} was slightly slower at higher pL, and in D_2O compared with H_2O. The average ratios at all potentials of the mean τ_{tail} data for essentially symmetrical pL are 1.31 (pD 8/pH 7.5), 1.04 (pH 7.5/pD 7), 1.23 (pD 7/pH 6.5), 1.05 (pH 6.5/pD 6), and 1.51 (pD 6/pH 5.5). The apparent slowing by D_2O was thus 23–51%, and some part of this effect may be ascribable to increasing pL_i.

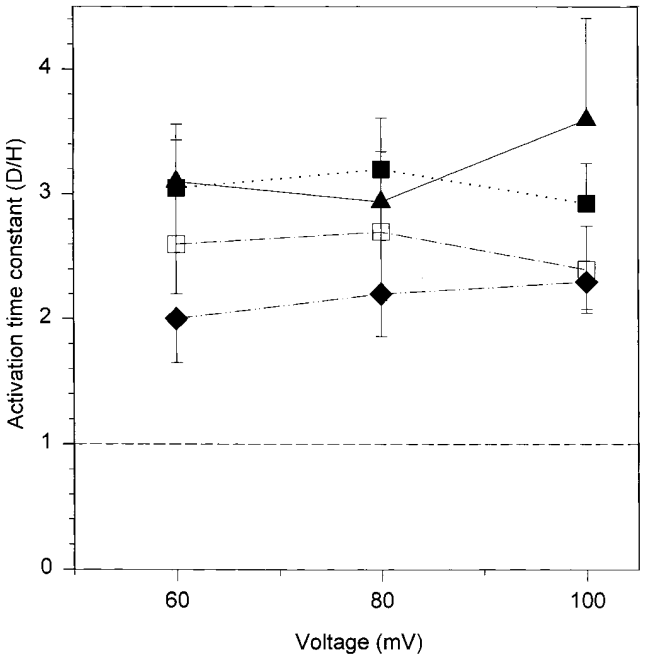

FIGURE 13. Slowing of activation by D_2O is illustrated as the ratio of τ_{act} measured in D_2O to that measured in the same cell in H_2O at effectively symmetrical pL. The effective pL in each case is 0.5 U higher in D_2O than in H_2O (see *Practical Considerations*). Symbols show the mean ± SEM of the ratio of pD_o 8 to pH_o 7.5 (▲), pD_o 7 to pH_o 6.5 (■), and pD_o 6 to pH 5.5 (◆). Fitting procedure and numbers of cells are given in Fig. 9 legend. Solid symbols are from experiments with D_2O pipette solutions; 4 cells studied at pD_o 7 and pH_o 6.5 with pH_i 6.5 (H_2O) in the pipette are also plotted (□). Data points are connected by lines and a reference line at a ratio of 1.0 is also plotted. There was no significant difference between mean ratios at different pD at any potential.

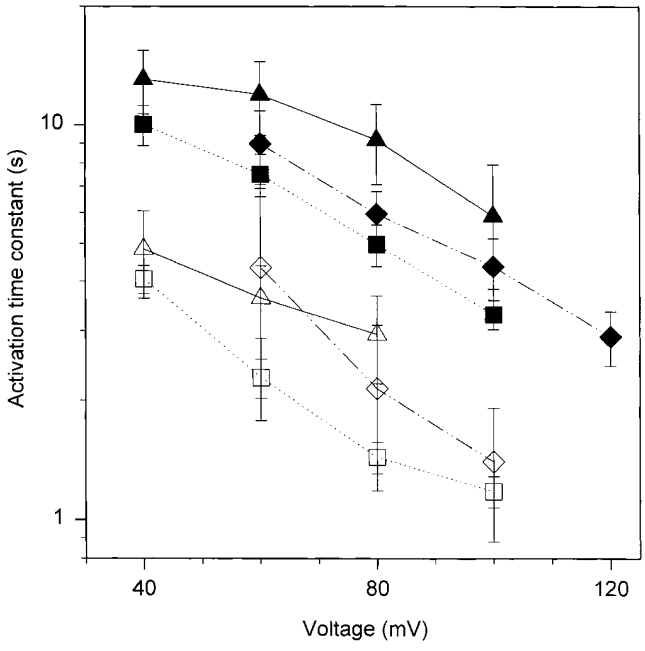

FIGURE 12. Average time constant of activation, τ_{act}, in H_2O (*open symbols*) and D_2O (*solid symbols*). Symbols show the mean ± SEM at pD 8//pD 8 in 5–7 cells (▲), pH_o 7.5//$pH_{i,eff}$ 7.5 in 5 cells (△), pD_o 7//pD 7 in 9–12 cells (■), pH_o 6.5//$pH_{i,eff}$ 6.5 in 7–9 cells (□), pD_o 6//pD 6 in 3–6 cells (◆), and pH_o 5.5//$pH_{i,eff}$ 5.5 in 4 cells (◇).

In some cells τ_{tail} is independent of pH_o (DeCoursey and Cherny, 1996*a*; Cherny et al., 1997), but the effects of pH_i have not been clearly determined. Therefore, we attempted to compare τ_{tail} in H_2O and D_2O at similar pL_i in the same cell by varying the NH_4^+ gradient. Increasing pH_i in individual cells at constant pH_o consistently slowed τ_{tail} by a small amount (not shown). When D_2O was compared with H_2O at a constant NH_4^+ gradient, i.e., at nearly constant pL_i (*see above*), there was also a consistent slowing of τ_{tail} in nearly every cell, by roughly 50%, consistent with the average values given above.

Deuterium effects in cell-attached patches. Fig. 15 illustrates putative H^+ currents in a cell-attached patch. The cell was bathed with isotonic $KMeSO_3$ solution to depolar-

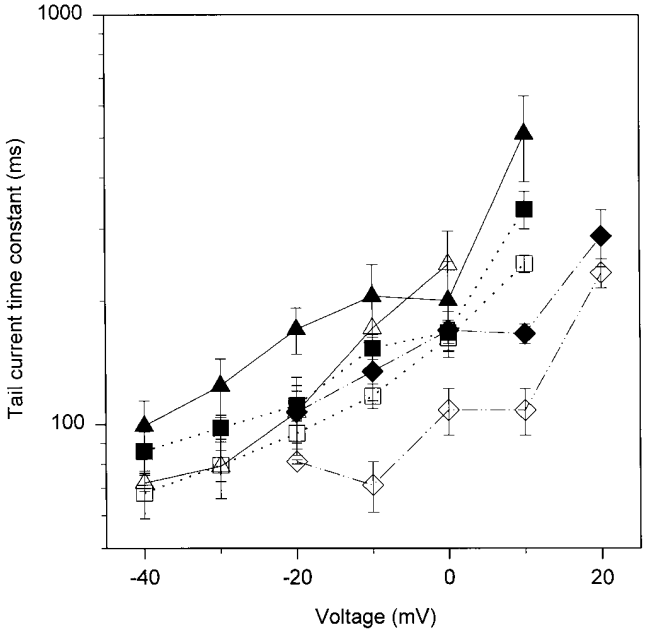

FIGURE 14. Tail current time constant, τ_{tail} at effectively symmetrical pH (*open symbols*) or pD (*solid symbols*). Symbols indicate pD_o 8.0//pD_i 8.0 (▲), pH_o 7.5//$pH_{i,eff}$ 7.5 (△), pD_o 7.0//pD_i 7.0 (■), pH_o 6.5//$pH_{i,eff}$ 6.5 (□), pD_o 6.0//pD_i 6.0 (◆), or pH_o 5.5//$pH_{i,eff}$ 5.5 (◇). Plotted is the mean ± SEM of τ_{tail} obtained by fitting the decay of the tail current with a single exponential (Eq. 3). Means are for 4–10 cells for each condition, with fewer measurements at some potentials.

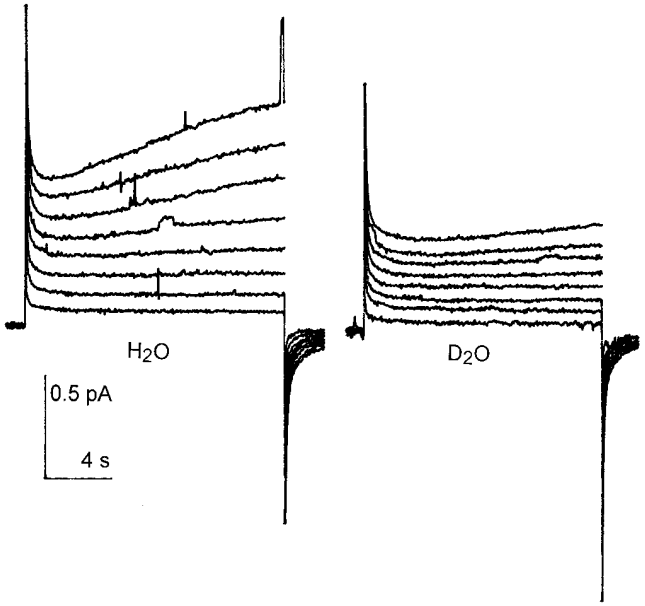

FIGURE 15. H^+ and D^+ currents in a cell-attached patch. During 16-s depolarizing pulses, there are slowly increasing outward currents, which we interpret as H^+ currents. In both parts V_{hold} was −60 mV relative to the membrane potential, and pulses were applied to −40 mV through +100 mV in 20-mV increments. The bath contained $KMeSO_3$ solution, intended to clamp the membrane potential to near 0 mV, and the pipette contained pD 8.0 solution. (*B*). When the bath was changed to D_2O instead of H_2O, the outward currents were much smaller and, if anything, even slower to activate. The H^+ currents are small, consistent with a small patch area and the membrane being near the pipette tip (cf. DeCoursey and Cherny, 1995). The completeness of exchange of solvent near the membrane cannot be determined, but the altered behavior when D_2O in the bath replaced H_2O suggests that the solvent near the membrane was changed substantially.

ize the membrane to near 0 mV. During depolarizations positive to 0 mV, there are slowly activating outward currents that resemble H^+ currents (cf. DeCoursey and Cherny, 1995), as well as brief discrete openings of some other channel(s). When H_2O in the bath was replaced with D_2O, the outward currents became much smaller and appeared to activate even more slowly. This isotope effect is comparable to the effects seen in whole-cell configuration, but larger than reported for other ion channels (Table III). Therefore, we conclude that the slowly activating outward currents were in fact H^+ currents.

Absolute H^+ or D^+ permeability of the cell membrane (not through proton channels). The "leak" current at subthreshold voltages usually decreased when D_2O replaced H_2O. However, it appears extremely unlikely that the leak is carried primarily by H^+ or D^+. Attempts to calculate the H^+ permeability, P_H, of the leak current using the Goldman-Hodgkin-Katz (GHK) current equation (Goldman, 1943; Hodgkin and Katz, 1949):

$$I_H = P_H z^2 \frac{EF^2}{RT} \frac{[H^+]_i - [H^+]_o \exp\frac{-zFE}{RT}}{1 - \exp\frac{-zFE}{RT}}, \qquad (5)$$

where I_H and P_H are expressed normalized to membrane area estimated assuming that the specific capacitance is 1 μF/cm², revealed numerous inconsistencies with this idea. The slope conductance of leak currents (defined as time-independent currents at subthreshold potentials) rarely changed by more than twofold/U change in pH or pD, and not always in the same direction. For a large pL gradient (e.g., pD 8//6), leak currents at negative potentials but positive to E_L were inward, giving a negative calculated P_L. Calculated values for P_L decreased substantially at low pL_o, even when the observed leak slope conductance was increased. Finally, the apparent reversal potential of the leak current, which was not well defined because the leak currents were often small, was usually closer to 0 mV than to E_L, and did not always change in the "right" direction when pL_o was varied. In summary, there is no evidence that H^+ carries a significant fraction of the leak current. An upper limit on the passive membrane permeability to H^+ or D^+ can be given as $<<10^{-4}$ cm/s at pH_i 5.5 or pD_i 6. By comparison, when the g_H is fully activated, P_H exceeds 1 cm/s at pH 8.0//7.5 (calculated from data in Cherny et al., 1995).

TABLE III

Deuterium Isotope Effects on Other Channels (temperature, °C)

Channel (permeant ion)	Conductance (H_2O/D_2O)	τ_{act} (D_2O/H_2O)	τ_{tail} (D_2O/H_2O)	τ_{inact} (D_2O/H_2O)	Reference
Na^+	1.22 (0–2)	1.4 (0–2)	1.39 (0–2)	1.86 (0–2)	Meves, 1974
Na^+	—	1.33 (9.5)	~1.0 (9.5)	>1 (95)	Alicata et al., 1990
Na^+	1.35 (2–4)	1.43 (2–4) 1.20 (12–14)	~1.0 (5–14)	1.5–2.6 (3–6) ~1.4 (11–14)	Schauf and Bullock, 1980, 1982
K^+	1.47 (2–4)	1.40 (2–4) 1.17 (12–14)			Schauf and Bullock, 1980
K^+_{Ca}	1.18 (?)				Pottosin et al., 1993
gramicidin (Li^+,Cs^+)	1.03,1.16 (20)				Tredgold and Jones, 1979
gramicidin (K^+, Rb^+, Cs^+, NH_4^+)	1.16 (25)				Andersen, 1983
gramicidin (H^+)	1.2–1.35 (22)				Akeson and Deamer, 1991
AchR	1.49 (12)		0.85 (12)		Lewis, 1985
cyclic nucleotide-gated	1.36 (20)				Root and MacKinnon, 1994
α-Toxin	1.13–1.2 (24)				Kasianowicz and Bezrukov, 1995
H^+ currents	1.9 (20)	~3 (20)	≤1.5 (20)	none	this study

Values listed for τ_{act} in some cases include time-to-half-peak or other measures of activation, τ_{tail} reflects deactivation as tail current decay or single-channel lifetime, t_{inact} is the inactivation time constant. Na^+ channel gating current kinetics were not affected by solvent substitution (Meves, 1974). The effects on channel gating kinetics are clear at low temperatures (<10°C), but decrease as temperature increases, vanishing by 15–20°C (Schauf and Bullock, 1982; Alicata et al., 1990).

DISCUSSION

The deuterium isotope effects observed provide information about H^+ permeation as well as the regulation of gating by protons (or deuterons). The main results are: (*a*) D^+ permeates proton channels. (*b*) The relative permeability of proton channels is $>10^8$ greater for D^+ than for TMA^+. (*c*) The H^+ conductance through proton channels is ~1.9 times that of D^+. (*d*) D^+ regulates the voltage dependence of H^+ channel gating much like H^+. (*e*) The threshold for activating the proton conductance is a linear function of V_{rev} and changes 40 mV/U change in ΔpH or ΔpD. (*f*) D^+ currents activate with depolarization ~3 times slower than H^+ currents, but deactivation is at most 1.5-fold slower in D_2O. (*g*) At least 5.4 equivalent gating charges move across the membrane field during proton channel opening in D_2O and in H_2O. (*h*) The upper limit of any proton leak conductance of the membrane of rat alveolar epithelial cells must be $<<10^{-4}$ cm/s. When the g_H is fully activated, P_H exceeds 1 cm/s.

Properties of Proton Channels

Proton channels are extremely selective. At high pD, the D^+ permeability was $>10^8$ greater than the TMA^+ permeability. The calculated permeability ratio P_{TMA}/P_D decreased as pD increased, by about 10-fold/U change in pD_i. Although a concentration dependent permeability ratio cannot be ruled out, it seems more reasonable to suppose that deviations of V_{rev} from E_D are due to imperfect control of pD, rather than to finite permeability of the channel to other ions. Several other H^+ channels have been reported to have comparably high selectivity for H^+, including the F_0 component of H^+-ATPase (Althoff et al., 1989; Junge, 1989) and the M2 viral envelope protein (Chizhmakov et al., 1996).

Protons rather than hydroxide ions carry the current. The substantially lower conductance of proton channels in D_2O than in H_2O suggests that the charge-carrying species is H^+ (or D^+) rather than OH^- (or OD^-). The isotope effect for D^+ is large because its mass is twice that of H^+, but OD^- is only 6% heavier than OH^-, and thus a much smaller isotope effect is to be expected: 41% for D^+ vs. 3% for OD^- for a classical square-root dependence on the mass of reactants (Glasstone et al., 1941). A similar argument can be made against H_3O^+ which would have a predicted isotope effect of just 8% over D_3O^+. However, the extremely high selectivity of the g_H has been ascribed to a Grotthuss-type or proton-wire permeation mechanism, which could exist for L^+ or OL^-, but not L_3O^+ (Nagle and Morowitz, 1978; DeCoursey and Cherny, 1994). Additional evidence supporting H^+ rather than OH^- as the charge carrying species is that the g_H increases ~1.7-fold/U decrease in pH_i over the range pH_i 7.5–4.0 (DeCoursey and Cherny, 1995, 1996*a*), i.e., as $[H^+]_i$ increases and $[OH^-]_i$ decreases and $[OH^-]_o$ remains constant. Finally, the reduction of outward current in cell-attached patches when the bath solvent is changed from H_2O to D_2O (Fig. 15), is consistent with L^+ efflux across the membrane from the cell to the pipette, but not OL^- influx from the pipette into the cell.

Voltage-gated H^+ and D^+ currents pass through channels, not the phospholipid bilayer membrane: the g_H is not a membrane leak. The finding that the voltage-activated and time-dependent H^+ conductance is clearly larger than the D^+ conductance provides further support for the idea that this conductance occurs through specialized membrane transporters, presumably proteins, and not simply through leaks in the bilayer. The conductance of phospholipid bilayers to D^+ is similar to that of H^+ (Perkins and Cafiso, 1986; Deamer, 1987; Gutknecht, 1987). The proton (or OH^-) permeability, P_H, of lipid bilayer membranes is several orders of magnitude higher than its permeability to other cations. Reported values for P_H vary widely, from 10^{-9} to $<10^{-3}$ cm/s in lipid bilayers and from 10^{-5} to 10^{-3} cm/s in biological membranes (reviewed by Deamer and Nichols, 1985). At least part of this variability is due to a dependence on the nature of the membrane and the pH gradient, ΔpH (Perkins and Cafiso, 1986)—at ΔpH = 1.0 in membranes of varying lipid composition, P_H ranged from 2.0×10^{-7} to 1.8×10^{-5} cm/s (Perkins and Cafiso, 1986). We suspect that no more than a very small fraction of our leak current at subthreshold potentials is carried by H^+ or D^+. This leak current provides an upper limit of $P_H << 10^{-4}$ cm/s in rat alveolar epithelial cells, providing no indication of any unusual H^+ permeability of these particular biological membranes. Even if the leak were carried entirely by H^+ or D^+, P_H increases by 3–4 orders of magnitude during depolarization from subthreshold to large positive potentials. It is difficult to imagine that a transient water-wire spanning the membrane would exhibit consistent, well-defined voltage- and time-dependent gating.

If we convert the observed voltage-gated H^+ current to permeability, P_H, using the GHK current equation (Goldman, 1943; Hodgkin and Katz, 1949), P_H increases with depolarization approaching a limiting value at any given ΔpH. However, the value calculated for P_H is much larger at high pH_i, because of the relative insensitivity of the H^+ conductance, g_H, to absolute pH (Cherny et al., 1995; DeCoursey and Cherny, 1995). The limiting value for P_H is about 1.1×10^0 cm/s at pH 8.0//7.5, 1.7×10^{-1} cm/s at pH 7.0//6.5, and 1.4×10^{-2} cm/s at pH 6.0//5.5 (recalculated from data in Cherny et al., 1995). Clearly, the GHK formalism is not a useful means of expressing P_H through the voltage-activated g_H, because its value is nowhere near being concentration-independent. That the P_H values obtained for the voltage-gated g_H are 3–9 orders of magnitude greater than those for H^+/OH^- conductivity through lipid bilayers makes it clear that the voltage-activated g_H requires a special transport molecule and cannot reasonably be ascribed to H^+ permeation through the phospholipid component of the cell membrane.

Deuterium Permeation

What is the rate-limiting step in H^+ permeation? The ratio of H^+ current to D^+ current was 1.65, 1.91, and 1.92 at pD 6, 7, and 8, respectively. Nearly all the H^+ that carry current during a depolarizing pulse are derived from buffer molecules that were protonated before the pulse (DeCoursey, 1991). If diffusion of protonated buffer to the channel were rate limiting, one would predict a smaller isotope effect on the conductance. Protonated or deuterated buffer should have almost identical diffusion coefficients. However, the 25% greater viscosity of D_2O than H_2O (Table I) would impede the diffusion of buffer molecules. That the g_H is reduced by almost 50% in D_2O is inconsistent with buffer diffusion being rate determining. We have shown recently that above 10 mM buffer there is negligible limitation of H^+ current by the diffusion of buffer at either side of the membrane (DeCoursey and Cherny, 1996*b*). In contrast, the smaller deuterium isotope effect on the conductance of most ion channels is consistent with diffusion of permeant ions being the rate-determining factor (Table III).

If H^+ permeation were set by the hydrodynamic mobility of H_3O^+, then the H^+/D^+ conductance ratio should similarly correspond with the relative viscosities and dielectric constants of H_2O and D_2O (Lengyel and Conway, 1983). In fact, the relative mobility of H^+ in H_2O to D^+ in D_2O is significantly larger, namely 1.41 compared with 1.17 for KCl in H_2O vs. D_2O at 20°C (interpolated from the data of Lewis and Doody, 1933), indicating that a more rapid transfer mechanism for H^+ exists, namely the "Grotthuss" mechanism in which protons hop from one water molecule to another. An isotope effect of 1.4–1.5 might therefore be expected if H^+ or D^+ conduction to the mouth of the pore were rate determining, or if permeation through the channel involved a mechanism like H^+ or D^+ diffusion in bulk water. Indeed, the relative conductance of H^+ to D^+ through gramicidin is of this magnitude, 1.34 at 10 mM L_3O^+, consistent with the approach of L_3O^+ to the channel being rate limiting, and 1.35 at 5 M L_3O^+ where the gramicidin channel current is saturated and the ratio presumably reflects that of permeation mechanism (Akeson and Deamer, 1991). The g_H/g_D ratio in voltage-gated H^+ channels was larger than can be accounted for by diffusion of either buffer or L_3O^+ molecules, strongly suggesting that the rate-determining step in permeation occurs in the channel itself. Furthermore, the larger isotope effect in voltage-gated channels than in gramicidin suggests that H^+ permeates by a different mechanism than gramicidin, in which H^+ is believed to hop across a continuous hydrogen-bonded chain of water molecules filling the pore (Myers and Haydon, 1972; Levitt et al., 1978; Finkelstein and Andersen, 1981; Akeson and Deamer, 1991). Perhaps voltage-gated H^+ channels are not simple wa-

ter-filled pores, but include amino acid side groups in the hydrogen-bonded chain, as proposed previously to account for their high selectivity and nearly pH-independent conductance (DeCoursey and Cherny, 1994, 1995; Cherny et al., 1995), by analogy with the proton wire mechanism proposed by Nagle and Morowitz (1978) to explain H^+ transport through the "proton channel" component of mitochondrial and chloroplast H^+-ATPases and bacteriorhodopsin. In summary, although the permeation of H^+ through gramicidin behaves in a manner consistent with the behavior of H^+ in bulk water solution, the permeation of H^+ through voltage-gated channels appear to behave differently.

To explain the apparent pH independence of the H^+ conductance of bilayer membranes, Nagle (1987) suggested that the rate-determining step might be the breaking of hydrogen bonds between water molecules. Applied to H^+ channel currents, the H^+ conductance might have an activation energy like that of hydrogen bond cleavage. The isotope effect for cleavage of an ordinary hydrogen bond in liquid water is ~1.4 (Walrafen et al., 1996). The observed ratio of H^+ to D^+ current, ~1.65–1.92, is significantly larger, suggesting that the rate determining step resides elsewhere. If a quantum-mechanical tunnel transfer within the pore were rate determining, then a much larger isotope effect would be expected, for example, 6.1 calculated for the relative mobilities calculated for tunnel transfers in water (Conway et al., 1956). Although H^+ tunneling may occur in the channel, it evidently is not rate limiting.

As discussed above, we imagine that the H^+ channel is not a water-filled pore but is most likely composed of some combination of amino acid side groups and water molecules linked together in a membrane-spanning hydrogen-bonded chain. Proton conduction is believed to occur by a Grotthuss or proton wire mechanism, which requires both hopping and reorientation steps (see INTRODUCTION; Nagle and Morowitz, 1978; Nagle and Tristram-Nagle, 1983). By analogy with ice, the mobility of the H^+ "ionic defect" is 6.4×10^{-3} $cm^2\ V^{-1}\ s^{-1}$ (at −5°C, Kunst and Warman, 1980), about an order of magnitude greater than the Bjerrum L defect mobility, 5×10^{-4} $cm^2\ V^{-1}\ s^{-1}$ (at 0°C, Camplin et al., 1978), suggesting that the turning step may be rate determining. However, proton transfer may be slower when it occurs between two dissimilar elements of the hydrogen-bonded chain. For example, proton transfer is slowed in mixed solvents because protons become effectively trapped by the solvent molecule with higher H^+ affinity (Lengyel and Conway, 1983). It is intriguing that the mobility of H^+ in ice exhibits a large isotope effect, 2.7 for H^+/D^+ at −5°C (Kunst and Warman, 1980). Furthermore, the reorientation of hydrogen bonds during proton transport in ice exhibits a H_2O/D_2O ratio of ~1.6 (at −10°C, Eigen et al., 1964), suggesting by analogy that the turning step for water which is constrained in a channel pore may exhibit a larger isotope effect than water in free solution. Although the rate-limiting step in H^+ permeation appears to occur within the conduction pathway, we cannot resolve whether the hopping or turning step is rate determining.

Are H^+ channels really ion channels? In Table IV deuterium isotope effects on various membrane transporters other than channels are listed. The precise values depend strongly on the conditions of the measurement, but in general it appears that more complex transport mechanisms exhibit stronger isotope effects on transport rates, >1.7, compared with <1.5 for ion channel permeation (Table III). This result strengthens the conclusion that the H^+ channel is not a simple water-filled pore, which was based on its high H^+ selectivity and nearly pH independent conductance. If voltage-gated H^+ channels are not water-filled pores, should they be considered ion channels at all? H^+ current does not require ATP or any counter-ion, so the only possibly more accurate term would be a carrier. The essential difference between a carrier and a channel is that each ion transported through a carrier requires a conformational change in the molecule which changes the accessibility of the ion from one side of the membrane to the other, whereas an open channel conducts ions without obligatory conformational changes. (Of course, there are significant interactions between conducted ions and the channel pore.) Biological channels also exhibit gating, without which they would simply be holes in the membrane. The voltage-gated H^+ channel exhibits well-defined time-, voltage-, and pH-dependent gating. That the conduction process involves protons hopping across a hydrogen-bonded chain seems a minor distinction. The two-stage hop-turn mechanism of the proton-wire (Nagle and Morowitz, 1978) could perhaps be described technically as alternating-access, in that the hydrogen-bonded chain must re-load after each H^+ conduction event. However, a hop-turn mechanism is also believed to occur when H^+ are conducted through gramicidin, in which the proton wire is composed entirely of water molecules, and there seems to be consensus that gramicidin is an ion channel, not a carrier. On balance, we prefer the term channel, but recognize that H^+ conduction by a proton wire (hydrogen-bonded chain) mechanism may bear some similarities to the alternating access mechanism which defines carriers and that H^+ channels may be unique among ion channels in not having a water-filled pore.

Deuterium Isotope Effects on Gating

Regulation of H^+ channel gating by pH. The rates of H^+ channel opening (activation) and closing (deactivation) are voltage dependent, both processes becoming

TABLE IV

Comparison of D^+ and H^+ Flux through Other Membrane H^+ Transporters

Transporter	Rate (H_2O/D_2O)	References
H^+-ATPase (F_0 component)	1.7	Althoff et al., 1989
H^+-ATPase (intact) at 30°C	1.7–5.6	Kotyk and Dvoráková, 1992
Bacteriorhodopsin D85E mutant	2.1–4.7, 6.2, 2.8 1.2–6.7, 4.6, 1.7	Cao et al., 1995
Na^+/H^+ antiport at 37°C	1.5*	Elsing et al., 1995
Bilayer permeability	~1	Perkins and Cafiso, 1986; Deamer, 1987; Gutknecht, 1987
Voltage-gated H^+ current	1.7–1.9	this study

Except where noted, measurements were done at room temperature (~20°C). The bacteriorhodopsin values reflect the range of inverse time constant ratios of several kinetic components of the photocycle, and the inverse of the time constants of H^+ release and uptake, respectively. *Measured in human leukocytes or rat hepatocytes; in neither case was the D_2O effect significant.

faster at large voltages. Byerly et al. (1984) found that increasing pH_i or lowering pH_o shifted the voltage dependence of activation kinetics of H^+ currents in snail neurons to more positive potentials but that lowering pH_o slowed activation more than could be explained by a simple voltage shift. Subsequent studies in a variety of cells leave the impression that both low pH_o and high pH_i slow activation somewhat more than expected for a simple voltage shift (Kapus et al., 1993; Cherny et al., 1995; DeCoursey and Cherny, 1996*a*), although in some cases a simple shift by pH_o was observed (Barish and Baud, 1984; DeCoursey and Cherny, 1995). Studied in inside-out membrane patches, increasing pH_i slowed activation by approximately fivefold/U in addition to shifting the voltage dependence of channel opening (DeCoursey and Cherny, 1995). The effects of pH on deactivation are substantially weaker than on activation. The voltage dependence of τ_{tail} was shifted at most 20 mV/U change in ΔpH in alveolar epithelial cells (Cherny et al., 1995). In THP-1 monocytes changing pH_o by 2 U had no detectable effect on τ_{tail} (DeCoursey and Cherny, 1996*a*). Here we report that H^+ current activation is slowed dramatically in D_2O whereas deactivation was barely affected.

Deuterium isotope effects on other channels. Deuterium isotope effects on several voltage-gated ion channels are summarized in Table III. Two features are noteworthy. Deuterium slows the opening rate of all channels studied, but the slowing is much greater for H^+ channels. For Na^+ or K^+ channels, τ_{act} is slowed only ~1.4-fold near 0°C, and this effect is halved at 10–14°C (~1.2-fold slowing) and undetectable 15–20°C (Schauf and Bullock, 1982; Alicata et al., 1990). The relatively subtle effects on τ_{act} of other channels have been ascribed to changing solvent structure (e.g., Schauf and Bullock, 1980, 1982). The effect on Na^+ channel inactivation is significantly larger, decreases at higher temperatures, and may reflect a different mechanism. Also remarkable is the solvent-insensitivity of deactivation, a result that appears to hold also for voltage-gated H^+ channels. It is conceivable that the greater deuterium sensitivity of activation than deactivation reflects some common principle of the mechanism of ion channel gating. However, the large isotope effect on H^+ channel activation seems to implicate a protonation/deprotonation reaction in gating, rather than a mechanism involving changes in solvent structure.

Deuterium isotope effects on H^+ channels. The opening rate of H^+ channels was 3.2, 3.1, and 2.2 times slower in D_2O at pD 8, pD 7, and pD 6, respectively. In contrast, the closing rate was slowed only 1.5-fold or less. In the model proposed to account for the regulation of the voltage dependence of gating by pH, the first step in channel opening is deprotonation at an externally accessible site on the channel, and the first step in channel closing is deprotonation at an internally accessible site (Cherny et al., 1995). If deprotonation at the external site were the rate-determining step in channel opening, then the observed slowing of τ_{act} could reflect an increase in the pK_a of this site in D_2O by 0.34–0.51 U. We give more weight to the larger D_2O effects, because factors such as H_2O contamination and the possibility that other deuterium-insensitive steps in gating may contribute to the observed kinetics would tend to diminish the size of the observed effect. We conclude that the pK_a of the external site most likely increases by ~0.5 U in D_2O. The pK_a of simple carboxylic and ammonium acids increases in D_2O by ~0.5–0.6 U, whereas the pK_a of sulfhydryl acids increases only 0.1–0.3 U (Schowen, 1977). The observed slowing of τ_{act} thus speaks against cysteine as the amino acid comprising the hypothetical site. We conclude that the modulatory site that governs the opening of H^+ channels is most likely a histidine, lysine, or tyrosine residue. The stronger D_2O isotope effect on activation than deactivation suggests that either the external and internal regulatory sites are chemically different, or the first step in channel closing occurs before deprotonation at the internal site.

One remarkable aspect of the data in Fig. 11 is that there is no suggestion of saturation of the relationship between V_{rev} and $V_{threshold}$. We previously reported saturation of the shift in the position of the g_H-V relationship above pH_o 8, with only a 10–20-mV shift between pH_o 8 and pH_o 9 (Cherny et al., 1995). In the present study, similar apparent saturation was observed, and extending the measurement to pH_o 10 resulted in no further shift relative to pH_o 9. However, we found that at

high pH_o, V_{rev} deviated substantially from E_H. In the previous study we felt that we could not resolve V_{rev} at pH_o 9 due to the rapid kinetics. Although tail currents at pH_o 9 or pH_o 10 were resolved less well than at lower pH_o, when we plot $V_{threshold}$ against the best estimate of V_{rev} (Fig. 11), the data fall on the linear relationship consistent with the other, better determined data points. It appears that there is an anomalous loss of control over pH_i at very high pH_o. It is difficult to imagine that pH_o is not well established by 100 mM buffer in the bath, and, assuming that V_{rev} reflects the true ΔpH, pH_i must increase a full unit when pH_o is changed from 9 to 10. One possibility is that some additional pH-regulating membrane transport process is working under these conditions. For example, a recently described Cl^-/OH^- exchanger (Sun et al., 1996) working "backwards" might exchange external OH^- for internal Cl^-, in spite of the rather low (4 mM) Cl^- concentration in the pipette solutions. Although we cannot explain the mechanism, the phenomenon merits further study. The lack of saturation complicates estimation of the pK_a of the putative regulatory protonation sites on H^+ channels.

Predicting the voltage dependence of the g_H in intact cells. The definition of $V_{threshold}$ is certainly arbitrary, because by using longer pulses, heavier filtering, and higher gain, it is possible to detect smaller and smaller currents, and ultimately $V_{threshold}$ has no precise theoretical meaning. Nevertheless, predicting the circumstances under which the g_H might be activated in vivo is facilitated by some estimate of $V_{threshold}$. The slope of the line in Fig. 11 for the H_2O data corresponds with a 40.0-mV shift/U change in ΔpH, if V_{rev} changes by 52.4 mV/U ΔpH, as reported previously (Cherny et al., 1995), or a 44.4 mV/U shift if V_{rev} changed according to E_H. The slope in D_2O was virtually identical. Thus the previous conclusion that the voltage-activation curve is shifted by ~40 mV/U change in ΔpH is in excellent agreement with the present data both in H_2O and in D_2O. We previously proposed that $V_{threshold}$ in intact cells could be predicted from the empirical relationship:

$$V_{threshold} = V_0 - 40\ (pH_o - pH_i)\ mV, \quad (6)$$

where V_0 was typically 20 mV, but varied substantially from cell to cell (Cherny et al., 1995). This relationship is based on the nominal ΔpH. Considering the remarkably linear relationship in Fig. 11 between $V_{threshold}$ and V_{rev}, we suggest that a more accurate prediction can be based of the true ΔpH, which we feel is reflected more closely by the observed V_{rev} than by the applied ΔpH. The new, improved relationship (in H_2O) is:

$$V_{threshold} = 0.76\ V_{rev} + 18\ mV. \quad (7)$$

This relationship is very similar to that described by Eq. 6, in predicting a ~40-mV shift in $V_{threshold}$/U change in ΔpH, and $V_{threshold}$ near +20 mV at symmetrical pH ($\Delta pH = 0$), but emphasizes the use of V_{rev} as the ultimate indication of the true ΔpH. The dotted reference line in Fig. 11 illustrates that $V_{threshold}$ is positive to V_{rev} over the entire voltage range studied. The regulation of the voltage-activation curve by ΔpH thus results in only steady-state outward currents throughout the physiological range.

We are grateful for constructive comments on the manuscript by Peter S. Pennefather, Duan Pin Chen, the reviewers, and Noam Agmon, who also generously provided preprints. The authors appreciate the excellent technical assistance of Donald R. Anderson, and thank Charles Butler for some determinations of the pK_a of buffers in normal and heavy water.

This study was supported by a Grant-in-Aid from the American Heart Association and by National Institutes of Health Research Grant HL-52671 to T. DeCoursey.

Original version received 27 November 1996 and accepted version received 27 January 1997.

REFERENCES

Agmon, N. 1995. The Grotthuss mechanism. *Chem. Phys. Lett.* 244: 456–462.

Agmon, N. 1996. Hydrogen bonds, water rotation and proton mobility. *J. Chim. Phys. (Paris).* 93:1714–1736.

Akeson, M., and D.W. Deamer. 1991. Proton conductance by the gramicidin water wire: model for proton conductance in the F_0F_1 ATPases? *Biophys. J.* 60:101–109.

Alicata, D.A., M.D. Rayner, and J.G. Starkus. 1990. Sodium channel activation mechanisms: insights from deuterium oxide substitution. *Biophys. J.* 57:745–758.

Althoff, G., H. Lill, and W. Junge. 1989. Proton channel of the chloroplast ATP synthase, CF_0: its time-averaged single-channel conductance as a function of pH, temperature, isotopic and ionic medium composition. *J. Membr. Biol.* 108:263–271.

Andersen, O.S. 1983. Ion movement through gramicidin A channels: studies on the diffusion-controlled association step. *Biophys. J.* 41:147–165.

Barish, M.E., and C. Baud. 1984. A voltage-gated hydrogen ion current in the oocyte membrane of the axolotl, *Ambystoma. J. Physiol. (Lond.).* 352:243–263.

Bell, R.P. 1973. The Proton in Chemistry. 2nd ed. Cornell University Press, Ithaca, NY. pp. 310.

Bernal, J.D., and R.H. Fowler. 1933. A theory of water and ionic solution, with particular reference to hydrogen and hydroxyl ions. *J. Chem. Phys.* 1:515–548.

Brooks, S.C. 1937. Osmotic effects of deuterium oxide (heavy water) on living cells. *Science (Wash. DC).* 86:497–498.

Byerly, L., R. Meech, and W. Moody. 1984. Rapidly activating hy-

drogen ion currents in perfused neurones of the snail, *Lymnaea stagnalis*. *J. Physiol. (Lond.)*. 351:199–216.

Camplin, G.C., J.W. Glen, and J.G. Paren. 1978. Theoretical models for interpreting the dielectric behavior of HF-doped ice. *J. Glaciology*. 85:123–141.

Cao, Y., L.S. Brown, J. Sasaki, A. Maeda, R. Needleman, and J.K. Lanyi. 1995. Relationship of proton release at the extracellular surface to deprotonation of the Schiff base in the bacteriorhodopsin photocycle. *Biophys. J.* 68:1518–1530.

Carter, E.P., M.A. Matthay. J. Farinas, and A.S. Verkman. 1996. Transalveolar osmotic and diffusional water permeability in intact mouse lung measured by a novel surface fluorescence method. *J. Gen. Physiol.* 108:133–142.

Cherny, V.V., L.M. Henderson, and T.E DeCoursey. 1997. Proton and chloride currents in Chinese hamster ovary cells. *Membr. Cell Biol.* In press.

Cherny, V.V., V.S. Markin, and T.E. DeCoursey. 1995. The voltage-activated hydrogen ion conductance in rat alveolar epithelial cells is determined by the pH gradient. *J. Gen. Physiol.* 105:861–896.

Chizhmakov, I.V., F.M. Geraghty, D.C. Ogden, A. Hayhurst, M. Antoniou, and A.J. Hay. 1996. Selective permeability and pH regulation of the influenza virus M2 channel expressed in mouse erythroleukemia cells. *J. Physiol. (Lond.)*. 494:329–336.

Collie, C.H., J.B. Hasted, and D.M. Ritson. 1948. The dielectric properties of water and heavy water. *Proc. Phys. Soc. (Lond.)*. 60: 145–160.

Conway, B.E., J. O'M. Bockris, and H. Linton. 1956. Proton conductance and the existence of the H_3O^+ ion. *J. Chem. Phys.* 24: 834–850.

Cross, P.C., and P.A. Leighton. 1938. Rapid exchange between deutero-ammonia and hydrazine. *J. Am. Chem. Soc.* 60:981–982.

Danneel, H. 1905. Notiz über ionengeschwindigkeiten. *Zeitschrift. Elektrochemie Angewandte Physikalische Chemie*. 11:249–252.

Deamer, D.W. 1987. Proton permeation of lipid bilayers. *J. Bioenerg. Biomembr.* 19:457–479.

Deamer, D.W., and J.W. Nichols. 1985. Mechanisms of proton-hydroxide flux across membranes. *In* Water and Ions in Biological Systems. A. Pullman, V. Vasilescu, and L. Packer, editors. Plenum Press, New York. 469–481.

Dean, J.A. 1985. Lange's Handbook of Chemistry. Thirteenth Edition, McGraw-Hill Book Company. St. Louis.

DeCoursey, T.E. 1990. State-dependent inactivation of K^+ currents in rat type II alveolar epithelial cells. *J. Gen. Physiol.* 95:617–646.

DeCoursey, T.E. 1991. Hydrogen ion currents in rat alveolar epithelial cells. *Biophys. J.* 60:1243–1253.

DeCoursey, T.E. 1995. Mechanism of K^+ channel block by verapamil and related compounds in rat alveolar epithelial cells. *J. Gen. Physiol.* 106:745–779.

DeCoursey, T.E., and V.V. Cherny. 1994. Voltage-activated hydrogen ion currents. *J. Membr. Biol.* 141:203–223.

DeCoursey, T.E., and V.V. Cherny. 1995. Voltage-activated proton currents in membrane patches of rat alveolar epithelial cells. *J. Physiol. (Lond.)*. 489:299–307.

DeCoursey, T.E., and V.V. Cherny. 1996*a*. II. Voltage-activated proton currents in human THP-1 monocytes. *J. Membr. Biol.* 152: 131–140.

DeCoursey, T.E., and V.V. Cherny. 1996*b*. Effects of buffer concentration on voltage-gated H^+ currents: does diffusion limit the conductance? *Biophys. J.* 71:182–193.

DeCoursey, T.E., and V.V. Cherny. 1997. Where is the rate-limiting step in permeation through voltage-gated proton channels? *Biophys. J.* 72:A108. (Abstr.).

DeCoursey, T.E., E.R. Jacobs, and M.R. Silver. 1988. Potassium currents in rat type II alveolar epithelial cells. *J. Physiol. (Lond.)*. 395: 487–505.

Eigen, M., and L. DeMaeyer. 1958. Self-dissociation and protonic charge transport in water and ice. *Proc. R. Soc. Lond., A*. 247:505–533.

Eigen, M., L. DeMaeyer, and H.-C. Spatz. 1964. Über das kinetische verhalten von protonen und deuteronen in eiskristallen. *Berichte der Bunsen-Gesellschaft für Physikalische Chemie*. 68:19–29.

Elsing, C., A. Hirlinger, E.L. Renner, B.H. Lauterburg, P.J. Meier, and J. Reichen. 1995. Solvent isotope effect on bile formation in the rat. *Biochem. J.* 307:175–181.

Finkelstein, A. 1984. Water movement through membrane channels. *Curr. Topics Membr. Transp.* 21:295–308.

Finkelstein, A., and O.S. Andersen. 1981. The gramicidin A channel: a review of its permeability characteristics with special reference to the single-file aspect of transport. *J. Membr. Biol.* 59:155–171.

Folkesson, H.G., M.A. Matthay, H. Hasegawa, F. Kheradmand, and A.S. Verkman. 1994. Transcellular water transport in lung alveolar epithelium through mercury-sensitive water channels. *Proc. Natl. Acad. Sci. USA*. 91:4970–4974.

Glasoe, P.K., and F.A. Long. 1960. Use of glass electrodes to measure acidities in deuterium oxide. *J. Phys. Chem.* 64:188–190.

Glasstone, S., K.J. Laidler, and H. Eyring. 1941. The Theory of Rate Processes: The Kinetics of Chemical Reactions, Viscosity, Diffusion and Electrochemical Phenomena. McGraw-Hill Book Co., New York. 611 pp.

Goldman, D.E. 1943. Potential, impedance, and rectification in membranes. *J. Gen. Physiol.* 27:37–60.

Good, N.E., G.D. Winget, W. Winter, T.N. Connolly, S. Izawa, and R.M.M. Singh. 1966. Hydrogen ion buffers for biological research. *Biochemistry*. 5:467–477.

Grant, E.H., and R. Shack. 1969. Complex permittivity of D_2O at 35 GHz over the temperature range 4-62.5°C. *Trans. Faraday Soc.* 65: 1519–1522.

Grinstein, S., R. Romanek, and O.D. Rotstein. 1994. Method for manipulation of cytosolic pH in cells clamped in the whole cell or perforated-patch configurations. *Am. J. Physiol.* 267:C1152–C1159.

Gutknecht, J. 1987. Proton conductance through phospholipid bilayers: water wires or weak acids? *J. Bioenerg. Biomembr.* 19:427–442.

Hardy, R.C., and R.L. Cottington. 1949. Viscosity of deuterium oxide and water in the range of 5° to 125°C. *J. Res. Natl. Bureau of Standards*. 42:573–578.

Hasegawa, H., T. Ma, W. Skach, M.A. Matthay, and A.S. Verkman. 1994. Molecular cloning of a mercurial-insensitive water channel expressed in selected water-transporting tissues. *J. Biol. Chem.* 269:5497–5500.

Hille, B. 1992. Ionic Channels of Excitable Membranes. 2nd ed. Sinauer Associates, Inc. Sunderland, MA. 607 pp.

Hodgkin, A.L., and B. Katz. 1949. The effects of sodium ions on the electrical activity of the giant axon of the squid. *J. Physiol. (Lond.)*. 108:37–77.

Hückel, E. 1928. Theorie der beweglichkeiten des wasserstoff- und hydroxylions in wässriger lösung. *Zeitschrift Elektrochemie Angewandte Physikalische Chemie*. 34:546–562.

Jarzynski, J., and C.M. Davis. 1972. The viscosity of water. *In* Water and Aqueous Solutions. Structure, Thermodynamics, and Transport Processes. R. A. Horne, editor. John Wiley and Sons, Inc., New York. 701–721.

Junge, W. 1989. Protons, the thylakoid membrane, and the chloroplast ATP synthase. *Ann. N Y Acad. Sci.* 574:268–285.

Kapus, A., R. Romanek, A.Y. Qu, O.D. Rotstein, and S. Grinstein. 1993. A pH-sensitive and voltage-dependent proton conductance

in the plasma membrane of macrophages. *J. Gen. Physiol.* 102: 729–760.

Kasianowicz, J.J., and S.M. Bezrukov. 1995. Protonation dynamics of the α-toxin ion channel from spectral analysis of pH-dependent current fluctuations. *Biophys. J.* 69:94–105.

Kirsch, J.F. 1977. Secondary kinetic isotope effects. *In* Isotope Effects on Enzyme-Catalyzed Reactions. W.W. Cleland, M.H. O'Leary, and D.B. Northrop, editors. University Park Press, Baltimore. 100–121.

Kotyk, A., and M. Dvoráková. 1992. Are proton symports in yeast directly linked to H^+-ATPase acidification? *Biochim. Biophys. Acta.* 1104:293–298.

Kunst, M., and J.M. Warman. 1980. Proton mobility in ice. *Nature (Lond.).* 288:465–467.

Lengyel, S., and B.E. Conway. 1983. Proton solvation and proton transfer in chemical and electrochemical processes. *In* Comprehensive Treatise of Electrochemistry. Vol. 5. Thermodynamic and Transport Properties of Aqueous and Molten Electrolytes. B.E. Conway, J.O'M. Bockris, and E. Yeager, editors. Plenum Press, New York. 339–398.

Levitt, D.G., S.R. Elias, and J.M. Hautman. 1978. Number of water molecules coupled to the transport of sodium, potassium and hydrogen ions via gramicidin, nonactin or valinomycin. *Biochim. Biophys. Acta.* 512:436–451.

Lewis, C.A. 1985. Deuterium oxide and temperature effects on the properties of endplate channels at the frog neuromuscular junction. *J. Physiol. (Lond.).* 85:137–156.

Lewis, G.N., and T.C. Doody. 1933. The mobility of ions in H^2H^2O. *J. Am. Chem. Soc.* 55:3504–3506.

Lewis, G.N., and P.W. Schutz. 1934. The ionization of some weak electrolytes in heavy water. *J. Am. Chem. Soc.* 56:1913–1915.

Meves, H. 1974. The effect of holding potential on the asymmetry currents in squid giant axons. *J. Physiol. (Lond.).* 243:847–867.

Myers, V.B., and D.A. Haydon. 1972. Ion transfer across lipid membranes in the presence of gramicidin A: the ion selectivity. *Biochim. Biophys. Acta.* 274:313–322.

Nagle, J.F. 1987. Theory of passive proton conductance in lipid bilayers. *J. Bioenerg. Biomembr.* 19:413–426.

Nagle, J.F., and H.J. Morowitz. 1978. Molecular mechanisms for proton transport in membranes. *Proc. Natl. Acad. Sci. USA.* 75: 298–302.

Nagle, J.F., and S. Tristram-Nagle. 1983. Hydrogen bonded chain mechanisms for proton conduction and proton pumping. *J. Membr. Biol.* 74:1–14.

Perkins, W.R., and D.S. Cafiso. 1986. An electrical and structural characterization of H^+/OH^- currents in phospholipid vesicles. *Biochemistry.* 25:2270–2276.

Pomès, R., and B. Roux. 1996. Structure and dynamics of a proton wire: a theoretical study of H^+ translocation along the single-file water chain in the gramicidin A channel. *Biophys. J.* 71:19–39.

Pottosin, I.I., P.R. Andjus, D. Vucelic, and G.N. Berestovsky. 1993. Effects of D_2O on permeation and gating in the Ca^{2+}-activated potassium channel from *Chara. J. Membr. Biol.* 136:113–124.

Roberts, N.K., and H.L. Northey. 1974. Proton and deuteron mobility in normal and heavy water solutions of electrolytes. *J. Chem. Soc., Faraday Transactions I.* 70:253–262.

Robinson, R.A., and R.H. Stokes. 1965. Electrolyte Solutions. 2nd ed. Butterworths, London. 571 pp.

Roos, A., and W.F. Boron. 1981. Intracellular pH. *Physiol. Rev.* 61: 296–434.

Root, M.J., and R. MacKinnon. 1994. Two identical noninteracting sites in an ion channel revealed by proton transfer. *Science (Wash. DC).* 265:1852–1856.

Schauf, C.L., and J.O. Bullock. 1980. Solvent substitution as a probe of channel gating in *Myxicola*: differential effects of D_2O on some components of membrane conductance. *Biophys. J.* 30:295–305.

Schauf, C.L., and J.O. Bullock. 1982. Solvent substitution as a probe of channel gating in *Myxicola*: effects of D_2O on kinetic properties of drugs that occlude channels. *Biophys. J.* 37:441–452.

Schowen, R.L. 1977. Solvent isotope effects on enzymic reactions. *In* Isotope Effects on Enzyme-Catalyzed Reactions. W.W. Cleland, M.H. O'Leary, and D.B. Northrop, editors. University Park Press, Baltimore. 64–99.

Sun, B., C.H. Leem, and R.D. Vaughan-Jones. 1996. Novel chloride-dependent acid loader in the guinea-pig ventricular myocyte: part of a dual acid-loading system. *J. Physiol.* 495:65–82.

Thomas, R.C. 1988. Changes in the surface pH of voltage-clamped snail neurones apparently caused by H^+ fluxes through a channel. *J. Physiol. (Lond.).* 398:313–327.

Tripathi, S., and E.L. Boulpaep. 1989. Mechanisms of water transport by epithelial cells. *Q. J. Exp. Physiol.* 74:385–417.

Tredgold, R.H., and R. Jones. 1979. A study of gramicidin using deuterium oxide. *Biochim. Biophys. Acta.* 550:543–545.

Walrafen, G.E., W.-H. Yang, Y.C. Chu, and M.S. Hokmabadi. 1996. Raman OD-stretching overtone spectra from liquid D_2O between 22 and 152°C. *J. Phys. Chem.* 100:1381–1391.